

THE DEVELOPMENT OF AN EXPLOSIVELY  
DRIVEN HYPERVELOCITY GAS GUN

PIFR-132

GPO PRICE \$ \_\_\_\_\_

CFSTI PRICE(S) \$ \_\_\_\_\_

Hard copy (HC) \$2.50

Microfiche (MF) .75

# 653 July 65

FACILITY FORM 602  
N66 32788  
(ACCESSION NUMBER) -  
75  
(PAGES)  
CR-76941  
(NASA CR OR TMX OR AD NUMBER)

(THRU)  
/  
(CODE)  
~~1~~  
(CATEGORY)

PHYSICS INTERNATIONAL CO.

2700 Merced Street, San Leandro, California 94577

THE DEVELOPMENT OF AN EXPLOSIVELY  
DRIVEN HYPERVELOCITY GAS GUN

PIFR-132

By E. T. Moore and C. S. Godfrey

August 18, 1965

FINAL REPORT

Prepared under Contract No. NAS w-978 by  
Physics International Company  
San Leandro, California

NATIONAL AERONAUTICS AND SPACE ADMINISTRATION  
Headquarters  
Washington, D. C.



ABSTRACT

N66-32788

The principal aim of the work performed under Contract NAS w -978 was to develop and test an explosively driven hypervelocity projector capable of accelerating 0.1 gm projectiles to the highest possible velocity. This effort included all the necessary analytical and theoretical calculations for design improvement, fabrication and assembly of the projectors, and a complete diagnostic and test program. A high-explosive containment tank and hypervelocity diagnostic facility was designed and built to aid in the development and testing of these hypervelocity projectors.

The following sections describe the development of two basic explosively driven hypervelocity guns. A conical hypervelocity gun was developed, and successfully accelerated intact projectiles to 4.15 km/sec. Projectile fragments were accelerated to velocities of approximately 12.2 km/sec. Concurrently, a linear hypervelocity gun was developed to systematically investigate launcher geometries, acceleration levels, projectile materials, and light gases to be used ultimately in the higher-performance conical guns. The linear gun accelerated intact projectiles to 7.92 km/sec and broken projectiles to 8.33 km/sec.

*Author*

## CONTENTS

	<u>Page</u>
I. INTRODUCTION	1
II. CONICAL HYPERVELOCITY GUNS	3
<u>Theory and Analysis of Operation</u>	3
<u>Experimental Results</u>	12
III. LINEAR HYPERVELOCITY GUNS	23
<u>Theory and Analysis of Operation</u>	23
<u>Experimental Results</u>	26
IV. DIAGNOSTIC TECHNIQUES	38
V. EXPLOSIVES FIRING FACILITY	50
VI. CONCLUSION AND RECOMMENDATIONS	61
REFERENCES	63
APPENDIX	64

## ILLUSTRATIONS

Figure		Page
1	Operation of Conical Hypervelocity Gun	4
2	Axial Acceleration of Gas by Liner of Figure 1	5
3	Results of Computer Calculation of Shot S-1	7
4	Radiograph of Intermediate Stage of Collapsing Metal Liner (Shot S-3)	8
5	Radiograph of Late Stage of Collapsing Metal Liner (Shot S-4)	9
6	Axial Acceleration of Gas Referred to Frame of Reference Moving with Phase Velocity $U_p$	10
7	Typical Hypervelocity Assembly Using Solid High Explosive	14
8	Typical Hypervelocity Assembly Using Liquid High Explosive	15
9	Launcher Geometries	16
10	Calculated Base Pressure for Two Different Expansions	18
11	Calculated Gas Kinetics and Projectile Acceleration for Two Different Lengths of Expansion Chambers	19
12	Experimental Data Obtained from Shot L-5	21
13	Radiograph of Projectile in Flight, Shot L-5	22
14	Operation of the Linear Hypervelocity Gun	24
15	Calculated Operation of Linear Reservoir Gun	28
16	Calculated Base Pressure During Acceleration of Polyethylene Projectile by a Linear Reservoir Gun	29
17	Shot CLG-2	31
18	Experimental Results of Shot CLG-4	32
19	Experimental Results of Shot CLG-6	33

Figure		Page
20	Calculated Position-Time and Base-Pressure-Time Histories of an Accelerated Reservoir Hypervelocity Projector Using a 15-cm Tapered Reservoir	37
21	Calculation Simulating Shot SP-1 as Fired with 7.5-cm Tapered Reservoir	39
22	Hypervelocity Gun Assembly for Conical Shot S-2	40
23	Hypervelocity Gun Assembly for Linear Shot CLG-4	41
24	0.032-Inch Self-Shorting Pin, Schematic and Operational Characteristics	43
25	Typical Photo Transistor Trace (Shot CLG-8)	44
26	Setup and Shot Radiographs of Shot CLG-9	45
27	Setup Radiograph of Conical Shot S-3	47
28	Typical Pin-Backup and Pressure Transducer Traces (Shot CLG-6)	48
29	Crater from Impact of 4.15 km/sec Nylon Projectile in Aluminum (Shot L-5)	51
30	High Explosives Firing Facility	52
31	Exterior View of the High Explosives Containment Facility	53
32	Vacuum Pumps used to Evacuate the High Explosives Containment Tanks	54
33	8-lb Containment Tank Arriving at High Explosives Facility	56
34	Interior View of 8-lb Containment Tank, Showing the Wooden Lining with Conical Shot L-9 in Place for Firing	57
35	Exterior View of 8-lb Containment Tank with Diagnostic Instrumentation in Place for Conical Shot L-9	58
36	Central and Diagnostic Area of High Explosives Facility	60
A-1	Schematic Representation of Leaky Piston	64

Figure		Page
A-2	Flow of Gas Through Stationary Orifice	65
A-3	Calculational Model of Leaky Piston	66
A-4	Results of Typical Calculation for Leaky Piston Performance	67-68

## TABLES

I	Experimental Results of Explosively Driven Conical Hypervelocity Guns	13
II	Experimental Results of Explosively Driven Conical Hypervelocity Guns	27

## I. INTRODUCTION

In the last decade, the interest in attainable velocities for aeroballistic studies has grown from 3 km/sec to 15 km/sec. The design of space vehicles has extended this interest to velocities of 60 km/sec for the investigation of space-impact phenomena. Considerable effort has been expended to obtain such velocities in the laboratory in order to determine the damage inflicted upon a spacecraft by meteoritic debris and to establish vulnerability levels for nuclear weapons. Equally as important is the investigation of the moon's surface. The most salient features of the lunar surface are the myriads of craters. While it is generally assumed that these craters are of meteoritic origin, relatively little is known about the processes which occur when a meteorite strikes, e.g., the energy expended, the efficiency of the process, and the relationships between the energy or momentum of the meteorite and crater dimensions. As projectile velocities approach meteoritic velocities, they provide a basis for understanding not only the lunar contour and its surface material, but the nature and origin of the processes which have operated on it. In the effort to obtain higher velocities, various hypervelocity projectors such as light gas guns, explosive projectors, electrodynamic accelerators, and electromagnetic accelerators have been used to accelerate projectiles of limited mass and geometry to equally limited velocities. Unfortunately, these techniques have not provided the ranges of mass and velocity required by space scientists. This means that space-impact information must be extrapolated far beyond the experimental data.

The use of chemical explosives as a primary energy source for hypervelocity projectors has received particular attention because of the low cost, high specific energy, and the rate at which this energy can be delivered. However, hypervelocity experiments using high explosives have not performed in proportion to the potential of this energy source. Gas guns which utilize the gaseous detonation products

of the explosive are restricted by the low sound speed in the relatively low-temperature and high-molecular-weight gases. Projectiles which are launched more directly by the explosive are subject to:

(1) high-amplitude, short-duration pressure pulses, leading to the destruction of the projectile, (2) inefficient use of the high explosive after the projectile is in motion, and (3) uncontrollable accelerations. For example, shaped charge techniques have been used to accelerate projectiles weighing between  $10^{-2}$  gm and 100 gm to velocities of 17.0 km/sec. However, the mass of the projectile is not completely reproducible due to the high launching accelerations which cause projectile breakup. It was the aim of this program to design and develop an explosively driven hypervelocity gun to surmount the limitations of earlier explosive projectors and more fully realize the potential of the high explosive.

The initial analytical and experimental effort was directed toward the development of the conical-shaped hypervelocity gun described in Section II. During these investigations it became apparent that the time and relatively high cost required for fabrication and assembly of these conical projectors made it difficult to systematically analyze and improve the design of the gun. As a result, concurrent development was begun of the explosively driven linear hypervelocity gun described in Section III.

While it was apparent that this linear gun did not have the potential of the conical projector, it accelerated projectiles intact to moderate velocities, and its operation could be analyzed quite well. Parametric modifications could be investigated quickly and at low cost, and the design improvements resulting from these investigations could then be used in the higher-potential conical projector. Furthermore, the data obtained with the linear gun provided much needed information concerning projectile material, light gases, maximum tolerable pressure profiles, and launcher designs for obtaining higher velocities.

Both the conical and linear hypervelocity guns are designed to convert the available chemical energy of an explosive into directed kinetic energy of the projectile. The conversion sequence is from the chemical energy to kinetic energy of a gas-containing metal liner, to kinetic and internal energy of a light gas, and finally to kinetic energy of the projectile. The introduction of an intermediate volume of light gas between the projectile and an explosively driven metal liner permits the pressure profile at the base of the projectile to be controlled, both in magnitude and duration. The development of these guns is further discussed in the following sections.

## II. CONICAL HYPERVELOCITY GUN

### Theory and Analysis of Operation

The operation of the conical hypervelocity gun is illustrated in Figures 1 and 2. The conical-shaped metal liner is initially filled with a light gas (He or H<sub>2</sub>) at one atmosphere. As the detonation front propagates around the metal liner, the resulting pressure radially accelerates the liner ( $t_2$ ,  $t_3$ , and  $t_4$  in Figure 1), which collapses along the axis with a collapse angle of  $\theta_c$ . The motion of this liner sends a shock wave into the light gas, which is then axially accelerated by the collapsing cone ( $t_5$ ,  $t_6$ , and  $t_7$  in Figure 2). The phase velocity of the point of collapse  $U_p$  is given in terms of the initial cone angle  $\theta_i$ , the collapse angle  $\theta_c$ , and the detonation velocity of the high explosive  $D$ , and expressed as

$$U_p = D \frac{\sin(\theta_c + \theta_i)}{\sin \theta_c}$$

It is interesting to note that in the limit as  $\theta_c$  approaches zero, the phase velocity approaches infinity. Under these conditions, however, the gas would obviously be trapped. Therefore, some collapse angle must exist below which the gas would be trapped and not axially accelerated. This angle must be found experimentally, since the extreme convergence of the metal liner produces instabilities in the differencing



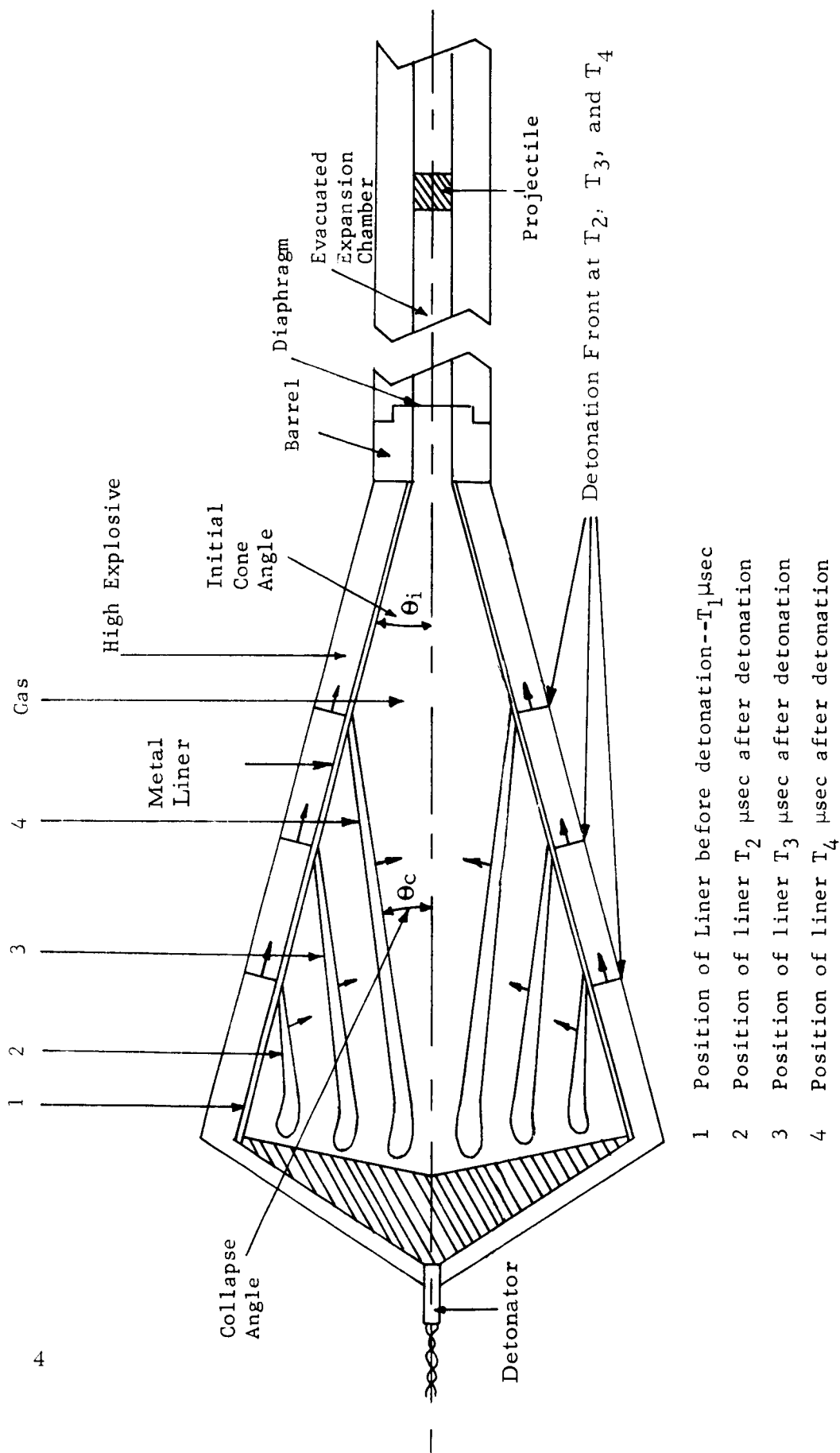
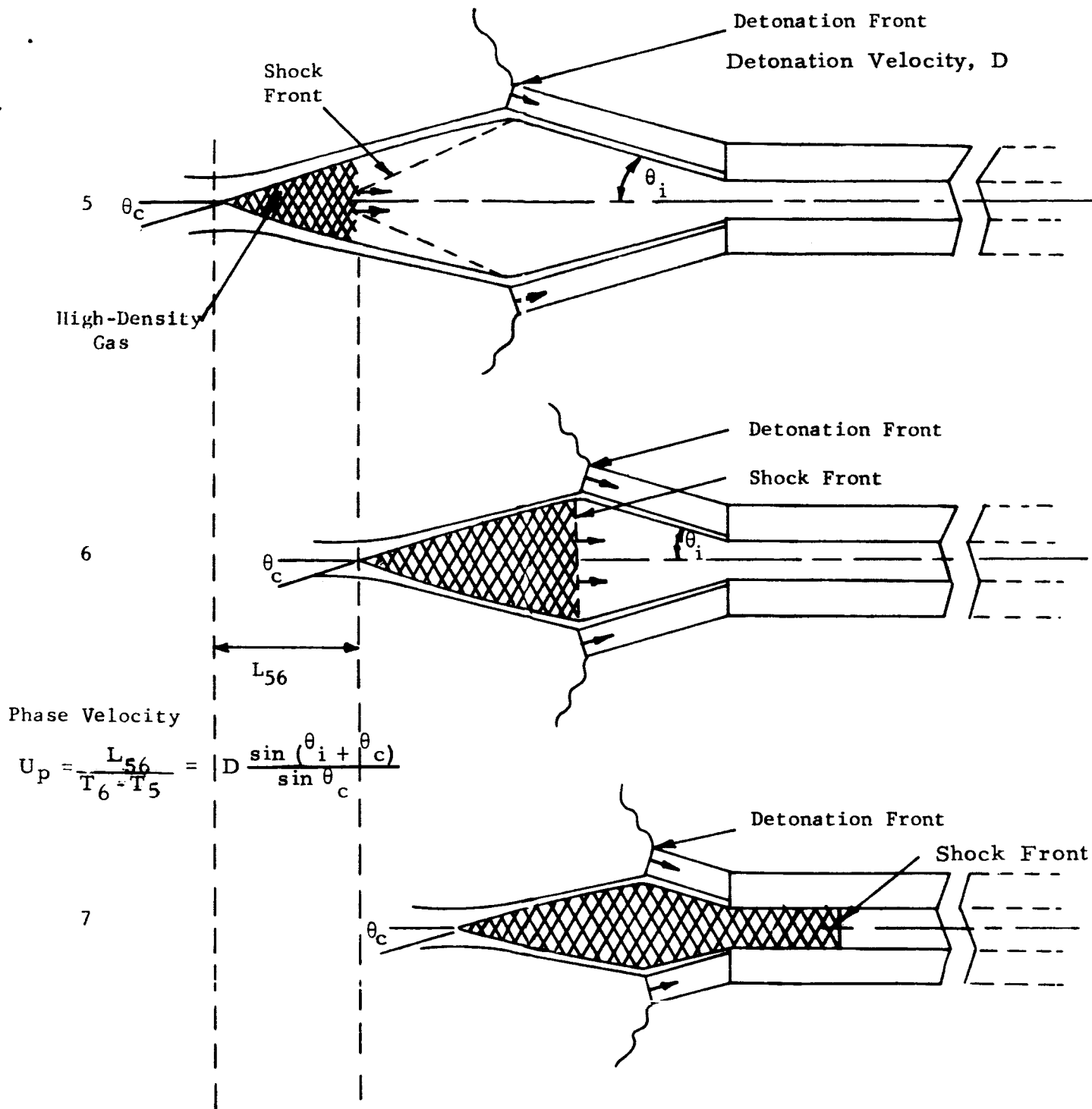


FIGURE 1. OPERATION OF CONICAL HYPERVELOCITY GUN



- 5 Position of liner  $T_5$   $\mu\text{sec}$  after detonation
- 6 Position of liner  $T_6$   $\mu\text{sec}$  after detonation
- 7 Position of liner  $T_7$   $\mu\text{sec}$  after detonation

FIGURE 2. AXIAL ACCELERATION OF GAS BY LINER OF FIGURE 1

equations used in a computer calculation. However, prior to the actual collapse of the liner, Physics International's two-dimensional, time-dependent, plastic-elastic computer code (PIPE)<sup>1</sup> was used to calculate the acceleration and subsequent motion of the conical liner by the solid explosive LX04-01. The problem was formulated in Lagrangian coordinates mocking up the assembly of the first solid explosive projector (S-1). This calculation shows the copper liner collapsing at an angle of 5.5 deg with a radial velocity of 3.3 km/sec. The results of this calculation are shown in Figure 3. The difference between the calculated and observed collapse angle (7.6 deg) is attributed to the lack of a realistic equation of state for this high explosive and the absence of the gas.

For a given initial cone angle and detonation velocity, the axial velocity of the collapsing cone (and hence the gas velocity) can be determined. For example, Figures 4 and 5 are radiographs showing the implosion of identical conical metal liners with initial angles of 16 deg (shots S-3 and S-4) at two different times. The liner was driven by the solid explosive LX04-01, which has a detonation velocity of 8.45 km/sec. The collapse angle was 11 deg, yielding an axial gas velocity of 20.4 km/sec. The radiographs of the implosion also provide geometrical data for obtaining the average compression of the gas. However, there are pressure and density gradients along the axis as gas is accelerated to the phase velocity  $U_p$  by the collapsing cone. Consider a frame of reference moving at the axial phase velocity  $U_p$  of the collapsing cone. In this frame of reference, the process resembles the simplified model shown in Figure 6. The conservation of momentum across the shock front shows that, for an ideal gas, the pressure in the shocked gas  $P_2$  is given by

$$P_2 = P_1 + \frac{\gamma + 1}{2} \rho_1 U_p^2$$

where  $P_1$  is the pressure ahead of the shock,  $\rho_1$  is the density of the gas ahead of the shock, and  $\gamma$  is the ratio of specific heats of the gas.

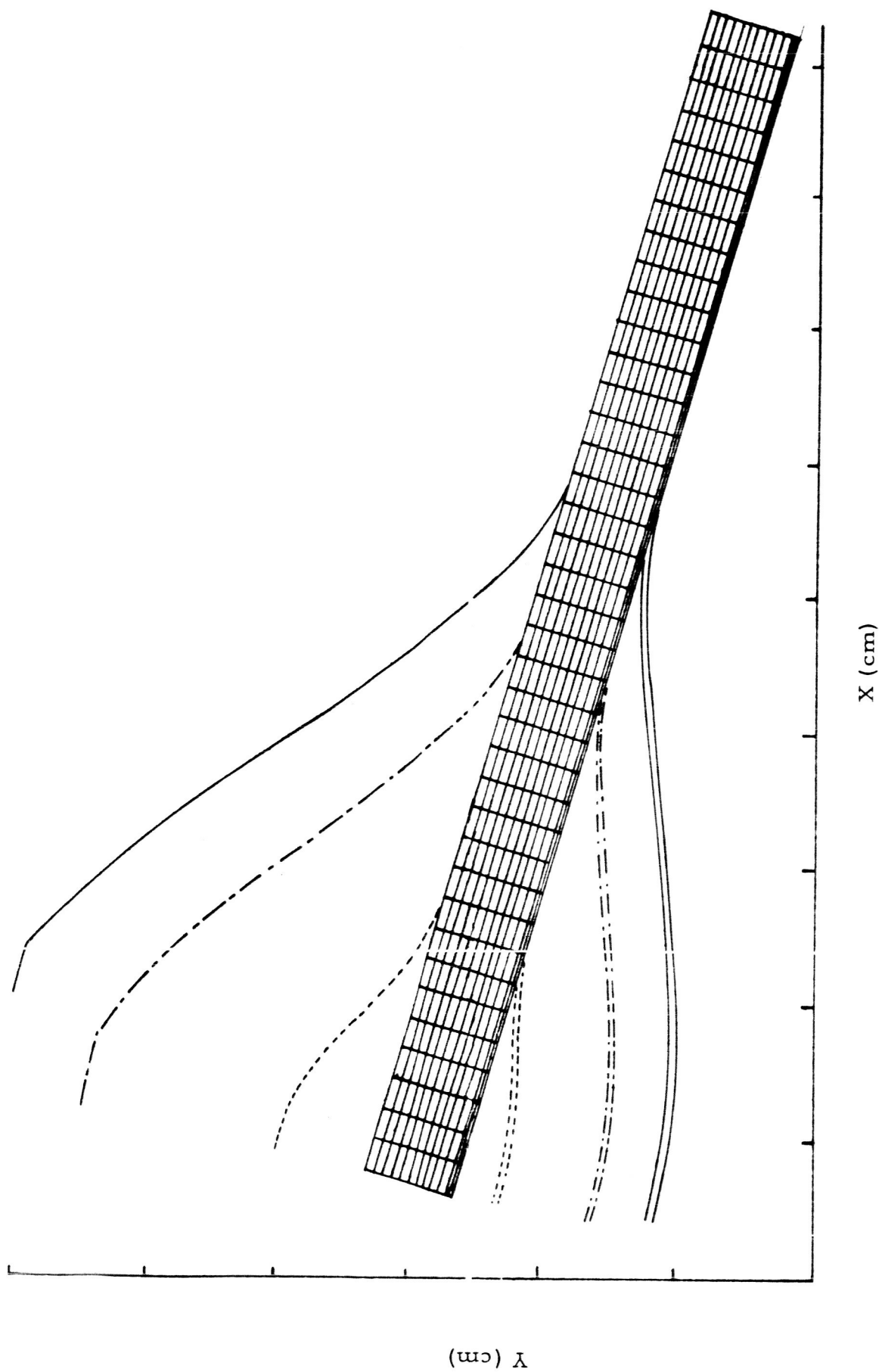


FIGURE 3. RESULTS OF COMPUTER CALCULATION OF SHOT S-1

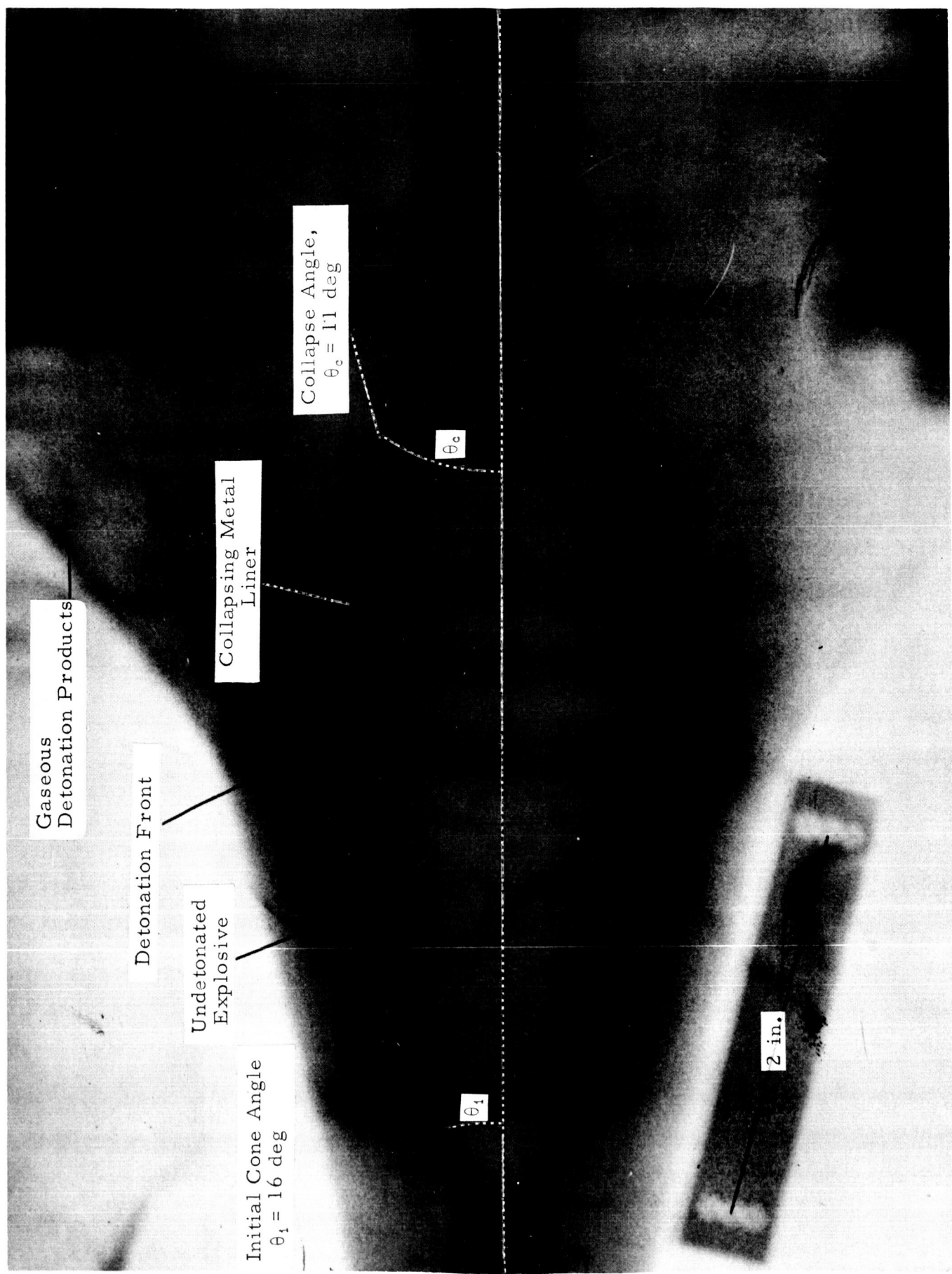


FIGURE 4. RADIOGRAPH OF INTERMEDIATE STAGE OF COLLAPSING METAL LINER (SHOT S-3)

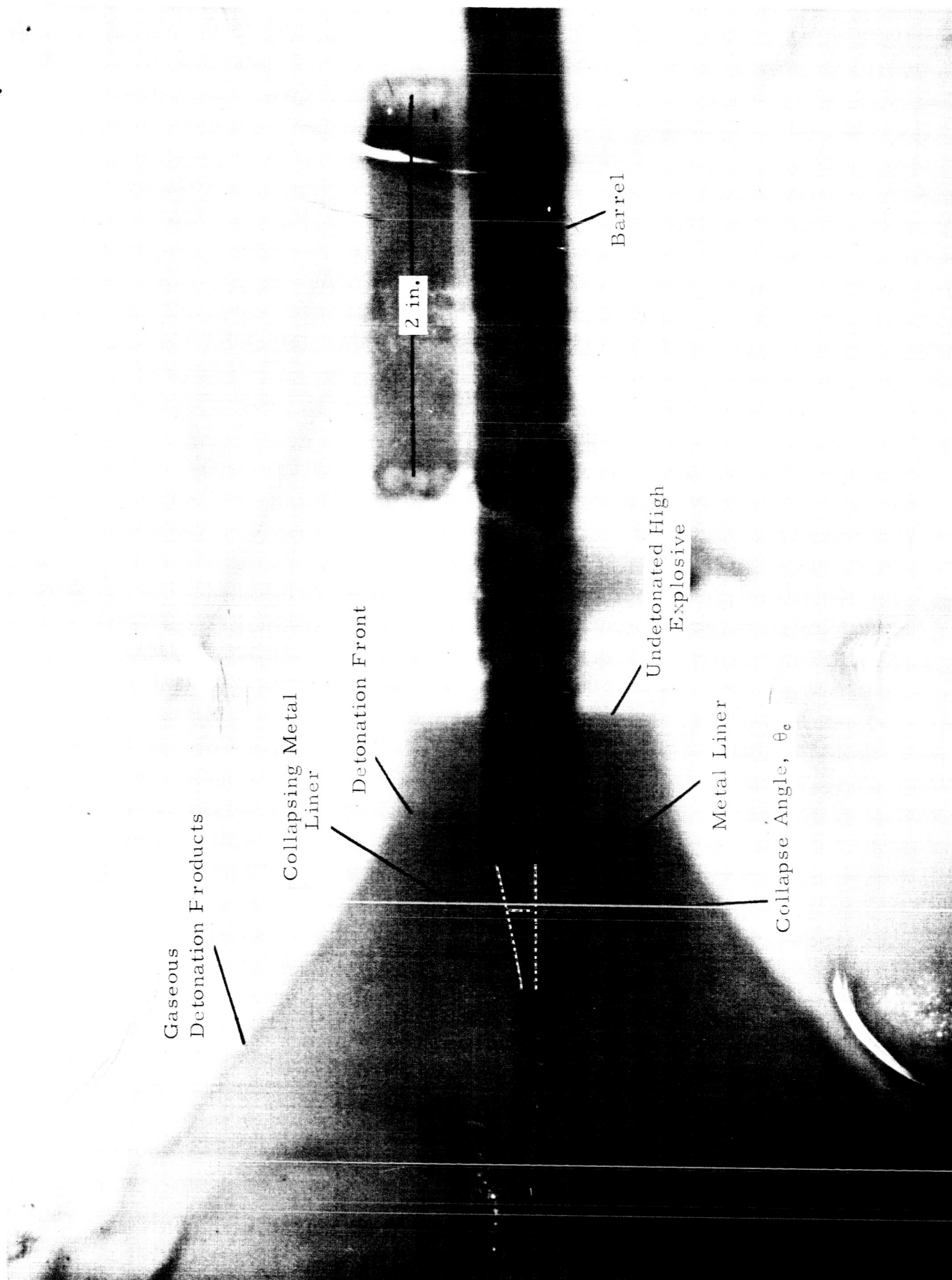
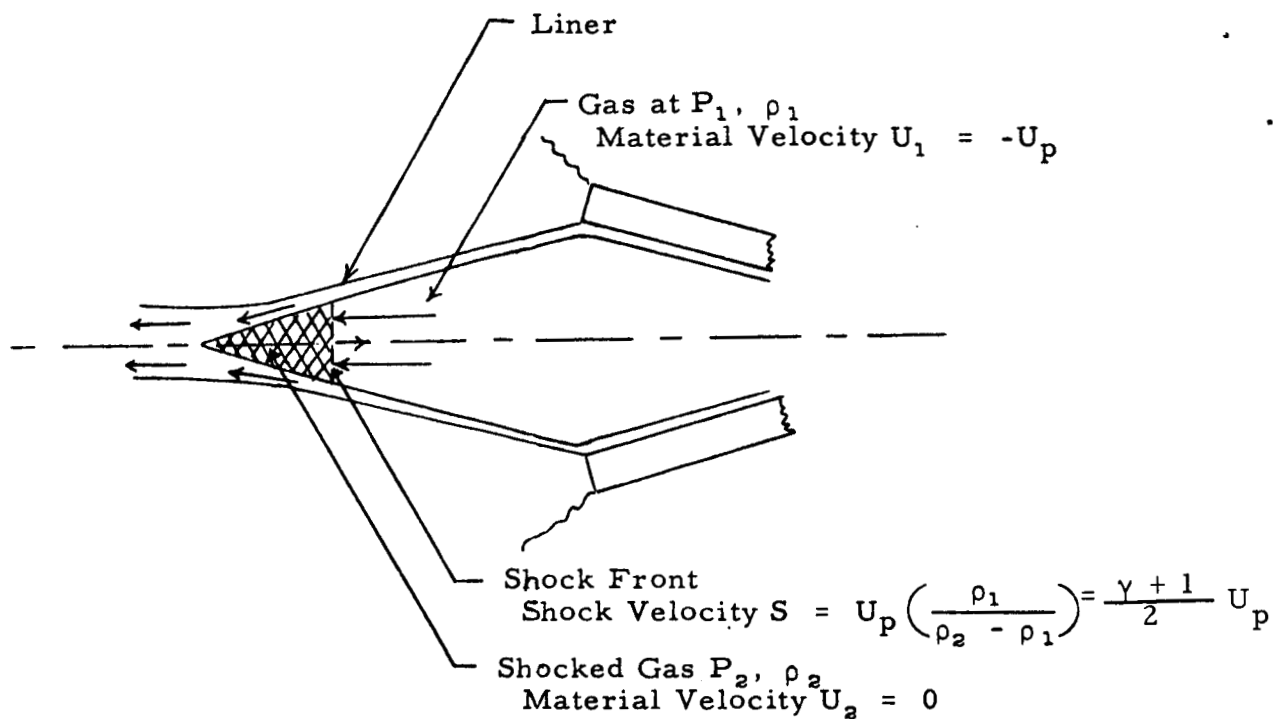
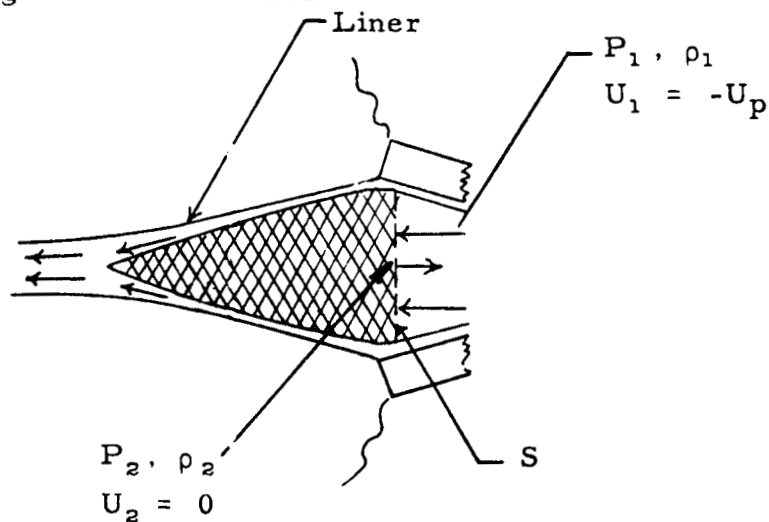


FIGURE 5. RADIOGRAPH OF LATE STAGE OF COLLAPSING METAL LINER (SHOT S-4)



a) Early stage of axial acceleration



b) Late stage of axial acceleration

FIGURE 6. AXIAL ACCELERATION OF GAS REFERRED TO FRAME OF REFERENCE MOVING WITH PHASE VELOCITY  $U_p$

For early stages of the axial acceleration, the gas near the collapsed point will have been shocked several times by the reflection of shock waves from the incoming liner; however, the gas near the apex of the uncollapsed cone will have been singly shocked. This causes axial gradients in the gas which may range from pressures on the order of 50 to 100 kb and densities of  $0.02$  to  $0.05 \text{ gm/cm}^3$  at the early point of collapse, to pressures of 1 to 5 kb and densities on the order of  $0.001 \text{ gm/cm}^3$  near the apex. The acceleration of a projectile by gradients such as these can be calculated by assuming a distribution of pressure, density, and particle velocities based on the preceding analysis, and by simulating these gradients in Physics International's one-dimensional, time-dependent Lagrangian hydrodynamic code (POD)<sup>2</sup> for parametric and design studies.

The configuration shown in Figure 1 appears to be similar to that used by Koski, et al.,<sup>3</sup> for obtaining fast metallic jets from the collapse of metal-lined cavities by high explosives. It might be expected, therefore, that the copper liner would form a metallic jet along the axis. However, Walsh, et al.,<sup>4</sup> showed that there is a critical collision angle for two colliding metal plates below which a jet will not form. Although these results cannot be applied directly to a collapsing conical liner, qualitatively one would expect a similar critical angle. No evidence of metal jets has been observed in the experiments. The high pressure developed in the gas also inhibits the formation of a jet from the metal liner.

The unique phasing produced by this geometry also characterizes the difference between the conical and linear hypervelocity projectors. As the initial cone angle approaches zero, the conical geometry approaches that of a cylinder, and the phase velocity (piston velocity) approaches the detonation velocity of the high explosive. The linear gun is described in Section III.



## Experimental Results

The main objective in the development of the conical hypervelocity gun was to utilize the extremely high gas velocities ( $\sim 30$  km/sec) and gas temperatures ( $\sim 5$  eV) provided by this design to launch a projectile. At the same time, guns using liquid and solid explosives were to be evaluated on a cost-versus-performance basis. Table I summarizes the results of the sixteen conical guns that have been fired during this program. Three different high explosives were used as drivers for the conical guns. The L-series of shots utilized the liquid explosive (NTN) which is a 5/1/1 mole ratio of nitromethane, tetranitromethane, and 1-nitropropane. This explosive was observed to have a detonation velocity of 6.72 km/sec at a density of  $1.24 \text{ gm/cm}^3$ . The S-series of shots utilized two different plastic-bonded HMX solid explosives, LX04-01 and PBHE. The LX04-01 was observed to have a detonation velocity of 8.45 km/sec at a density of  $1.86 \text{ gm/cm}^3$ . Due to the high cost ( $\sim \$500$ ) of obtaining the conical-shaped pieces of LX04-01 during the program, it was concluded that future guns would use the low-cost liquid explosive. However, the development of PBHE by Amcel permits replacement of the highly toxic liquid NTN by this castable solid. The reduced cost of fabricating and handling the complete solid-explosive hypervelocity gun assemblies more than compensates for the higher cost of PBHE ( $\sim \$125$  per assembly). This will be further reduced when Physics International's high-explosive casting facilities become operational.

Typical conical hypervelocity guns using solid and liquid explosives are shown, respectively, in Figures 7 and 8. The two launcher geometries which have been studied most extensively for these guns are shown in Figure 9. In the direct acceleration geometry, (Figure 9a), the projectile is located in the breech of the barrel (at the apex of the conical metal liner) and is directly subjected to the pressure profile from the radial compression and axial acceleration of the light gas by the collapsing cone. Shots L-1, L-2, L-4, S-1, and S-3 were of

TABLE 1. EXPERIMENTAL RESULTS OF EXPLOSIVELY DRIVEN CONICAL HYPERVELOCITY GUNS

Shot No.	Experiment	Explosives		Gas		Barrel		Projectile			Velocity ft/sec	Projectile Condition	Remarks			
		Weight (lb)	Type	Type	Pressure (psia)	Diam. (in.)	Length (in.)	Material	Diam. (in.)	Length (in.)				Mass (gm)		
L-1	Implosion angle	2.1	NTN	helium	29.7	0.20	12	HDPE	0.225	0.15	0.085	5.6	18,300	Broken	Radiograph obscured by lead blow-off gases <u>Fired 7/23/64</u>	
L-2	Implosion angle	2.1	NTN	helium	29.7	0.229	12	Lexan	0.229	0.17	0.132	5.9	19,300	Broken	Radiograph fair <u>Fired 8/6/64</u>	
L-3	Effect of slide plane	2.1	NTN	helium	29.7	---	--	---	---	---	---	---	---	---	---	Radiograph good <u>Fired 8/25/64</u>
S-1	Implosion angle 0.019 in. cone	1.95	LX04-1	helium	29.7	0.200	6	Lexan	0.200	0.15	0.104	---	---	Vaporized	Radiograph good, showed liner too thick <u>Fired 9/16/64</u>	
L-4	Launch Lexan projectile	1.5	NTN	helium	29.7	0.226	6	Lexan	0.226	0.180	0.139	---	---	Vaporized	<u>Fired 9/28/64</u>	
S-2	Implosion angle 0.011 in. cone	1.95	LX04-1	helium	14.7	0.215	6	Lexan	0.215	0.150	0.108	---	---	Vaporized	X-ray triggered early <u>Fired 10/14/64</u>	
S-3	Implosion angle 0.011 in. cone	1.95	LX04-1	helium	14.7	0.221	6	carbon	0.221	---	0.165	---	---	Vaporized	Radiograph good <u>Fired 11/3/64</u>	
S-4	50-cm Expansion chamber	1.95	LX04-1	helium	14.7	0.170	6	nylon	0.170	0.096	0.044	>1.2	>3,900	Good	<u>Fired 12/15/64</u>	
P-1	8-lb Gun, 30-cm Expansion chamber	11.3	NTN	helium	14.7	0.214	6	nylon	0.214	0.214	0.144	3.07	10,500	Good	<u>Fired 1/15/65</u>	
L-5	15-cm Expansion chamber	1.5	NTN	helium	14.7	0.170	6	nylon	0.170	0.085	0.034	4.15	13,700	Good	<u>Fired 1/26/65</u>	
L-6	5-cm Expansion chamber	1.5	NTN	helium	14.7	0.170	10	nylon	0.170	0.087	0.037	---	---	Vaporized	<u>Fired 1/28/65</u>	
L-7	Aluminum model	1.5	NTN	helium	14.7	0.170	10	aluminum	0.170	0.085	0.092	---	---	Vaporized	<u>Fired 2/5/65</u>	
L-8	Repeat L-5	1.5	NTN	helium	14.7	0.170	6	nylon	0.170	0.085	0.032	---	---	Vaporized	<u>Fired 2/16/65</u>	
L-9	Conical-linear combination	3.5	NTN	helium	14.5	0.177	12	nylon	0.184	0.094	0.043	---	---	Vaporized	<u>Fired 4/16/65</u>	
S-5	Sapphire spheres-- drag	1.8	PBHE	helium	16.0	0.177	6	sapphire	0.04	sphere	0.0021	8.95	29,400	Uncertain	Drag concept investigated <u>Fired 5/3/65</u>	
L-10	Reservoir	1.5	NTN	helium	14.5	0.14	5	HDPE	0.145	0.072	0.0195	---	---	Vaporized	Reservoir concept investigated <u>Fired 5/20/65</u>	

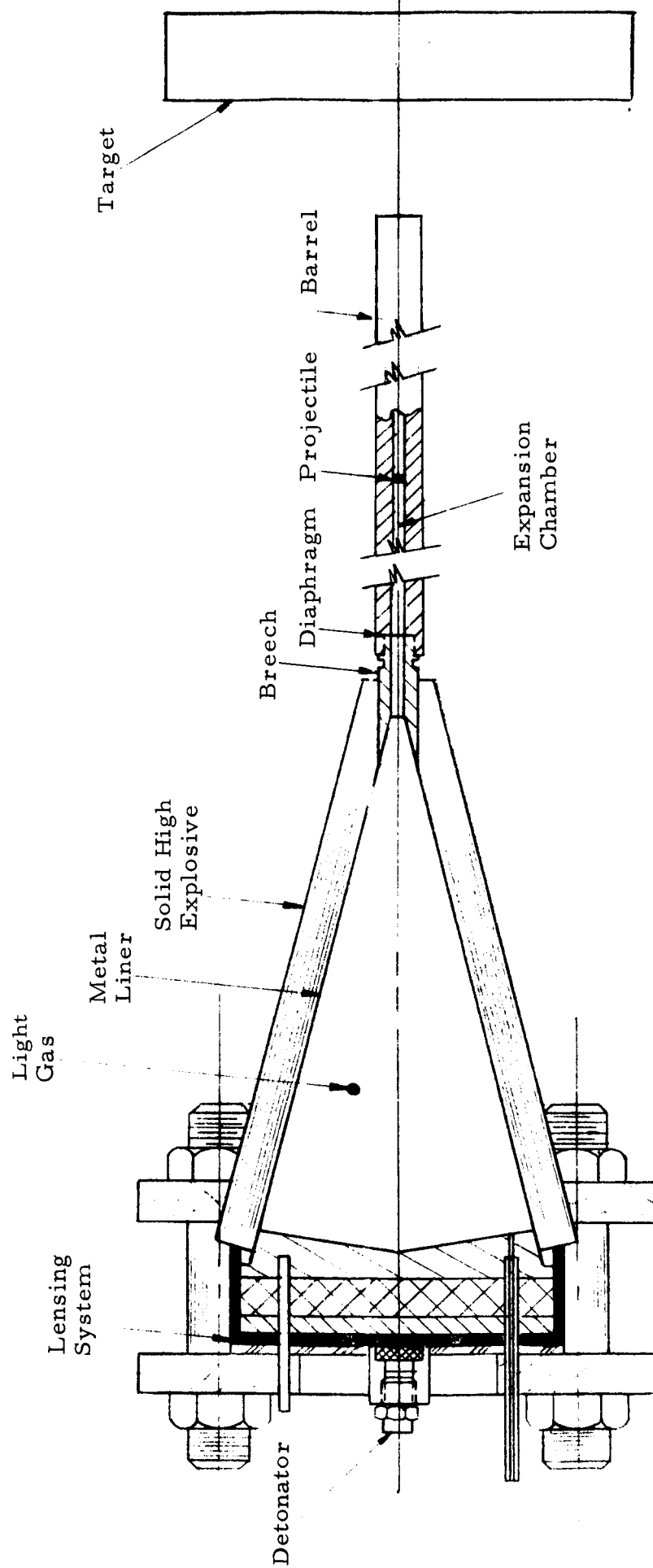


FIGURE 7. TYPICAL HYPERVELOCITY ASSEMBLY USING SOLID HIGH EXPLOSIVE

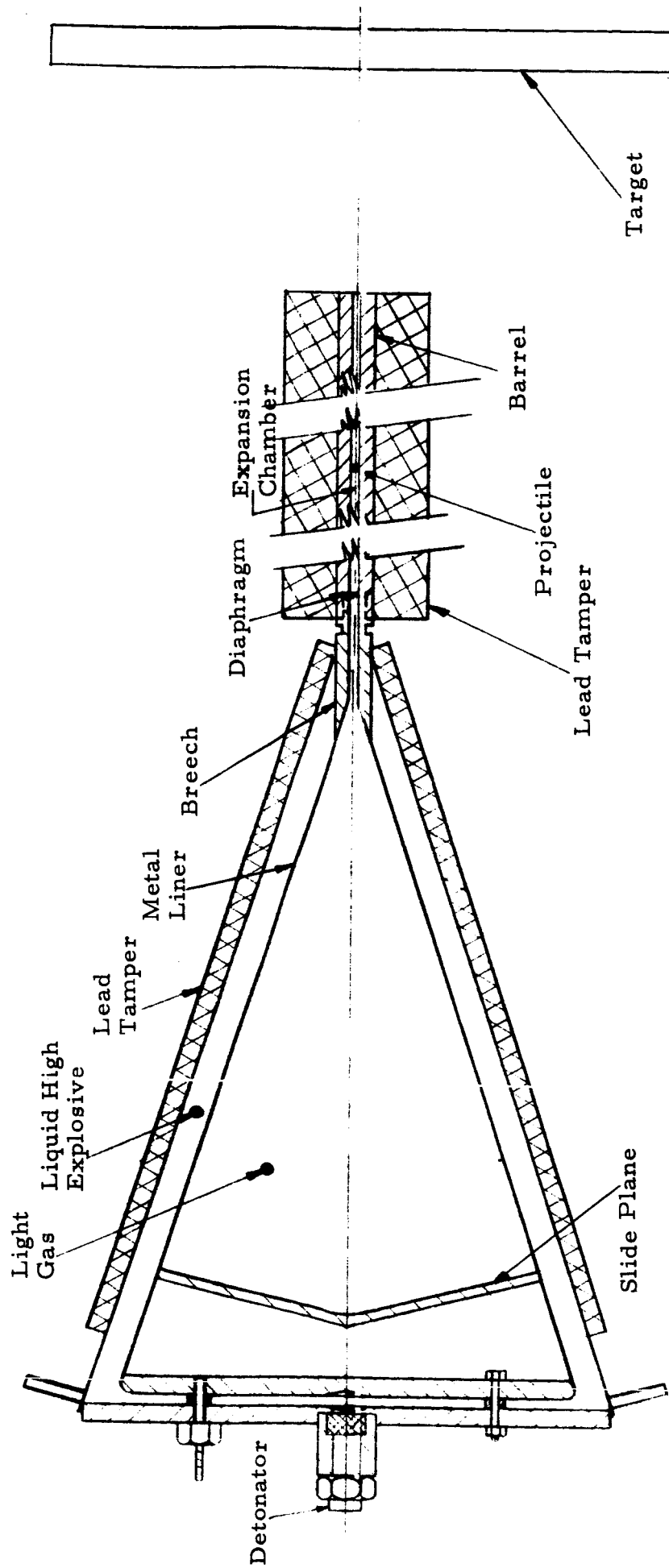


FIGURE 8. TYPICAL HYPERVELOCITY ASSEMBLY USING LIQUID HIGH EXPLOSIVE

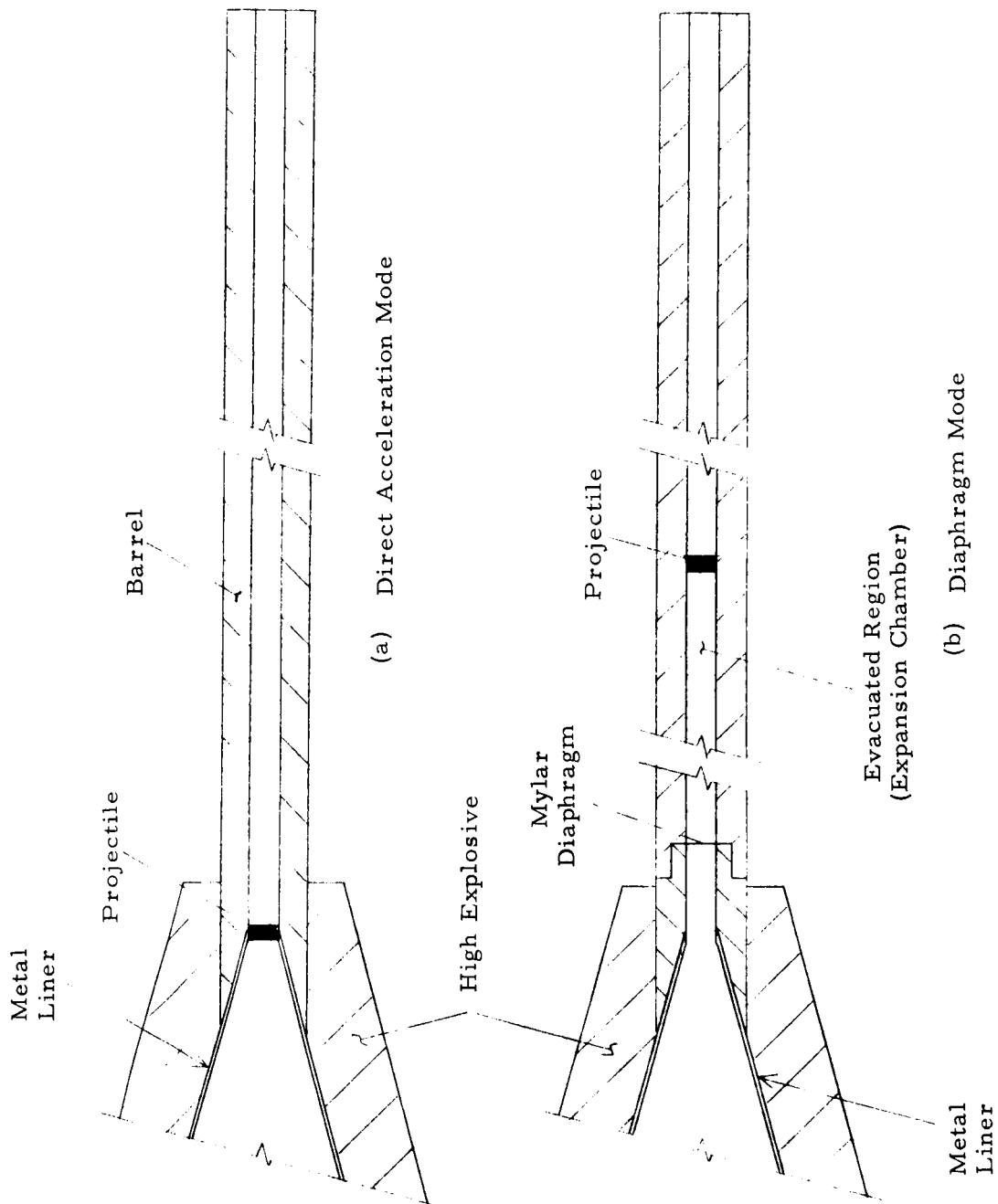


FIGURE 9. LAUNCHER GEOMETRIES

this type. The various projectile materials used in this geometry were high-density polyethylene (L-1), zelux "M" (L-2, L-4, S-1), aluminum (L-7), and carbon (S-3). The projectiles launched with this geometry were characteristically broken into several pieces or completely vaporized. The velocities of projected fragments were in the neighborhood of 6.0 km/sec whereas the velocity of the vaporized materials ranged from 24 to 30 km/sec. Even though the shots using the direct acceleration geometry did not produce intact projectiles, the data obtained from this series experimentally verified the operation of the gun. They also provided empirical relationships between the initial cone angle and collapse angle for a given explosive system. The projectile breakup and destruction was postulated to have been caused either by severe accelerations or radiation-initiated instabilities.

A parametric study was made using the one-dimensional hydrodynamic computer code (POD) to determine methods for lessening the severity of projectile acceleration. The pressure-time history in Figure 10 shows the results of placing an evacuated region (expansion chamber) of two different lengths between the gas and projectile. This permits a rarefaction to reduce the peak pressures and lengthen the duration of the pressure profile. The acceleration of projectiles corresponding to the two different expansion chamber lengths is shown in the position-time history of Figure 11. This study led to the diaphragm geometry of Figure 9b, in which a 0.002-in Mylar diaphragm was located in the breech of the barrel, creating an expansion chamber between the gas and projectile. Shots S-2, S-4, LP-1, L-5, L-6, L-7, and L-8 utilized this geometry. Shot S-2 used a zelux "M" projectile and a 9-cm expansion chamber, which resulted in the breakup of the projectile. However, experiments with the linear gun showed that nylon was a better projectile material for the types of acceleration obtained in an explosively-driven gun. Shot S-4 was then fired using a nylon

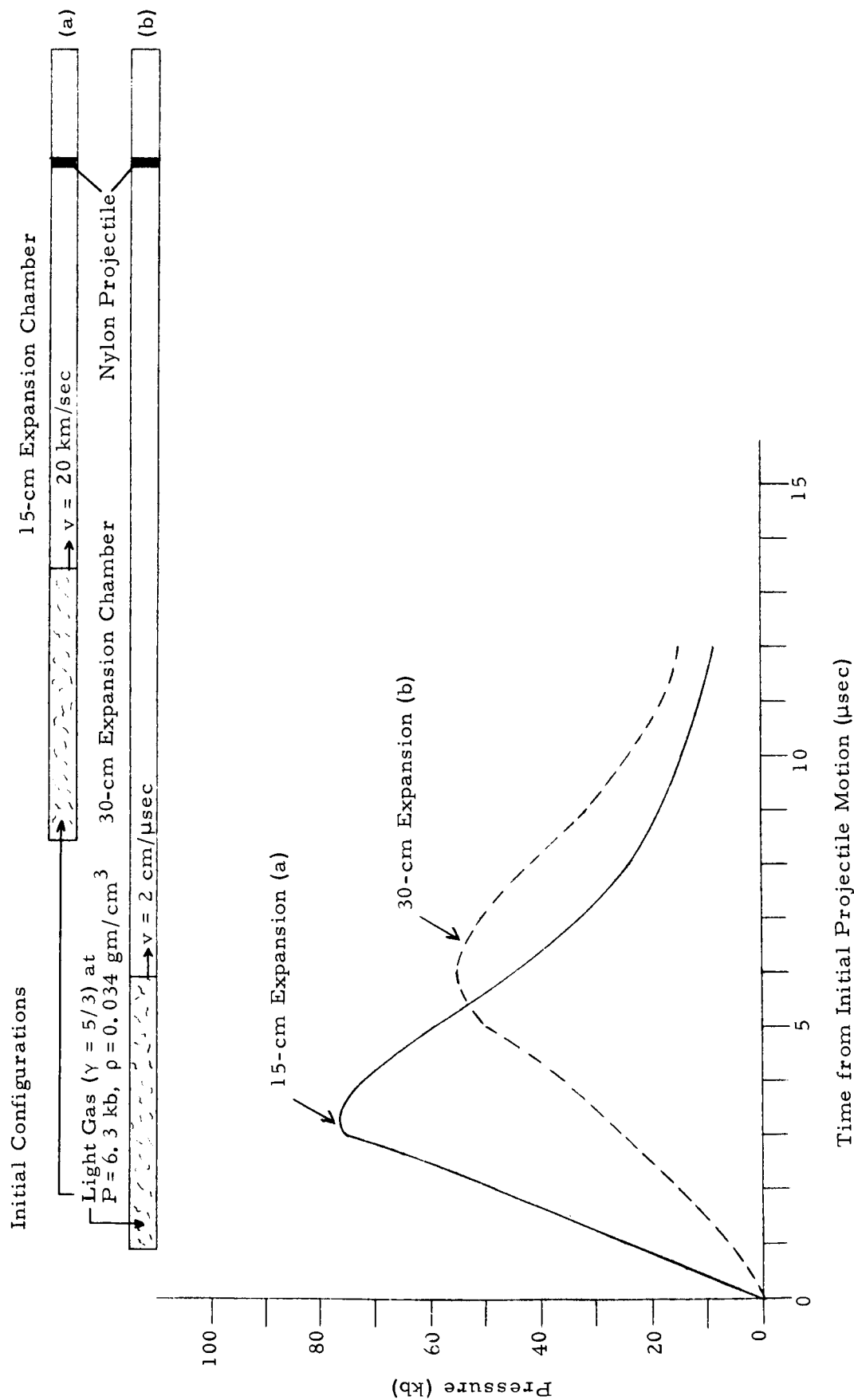


FIGURE 10. CALCULATED BASE PRESSURE FOR TWO DIFFERENT EXPANSIONS

Same Initial Configuration as Shown in Figure 10

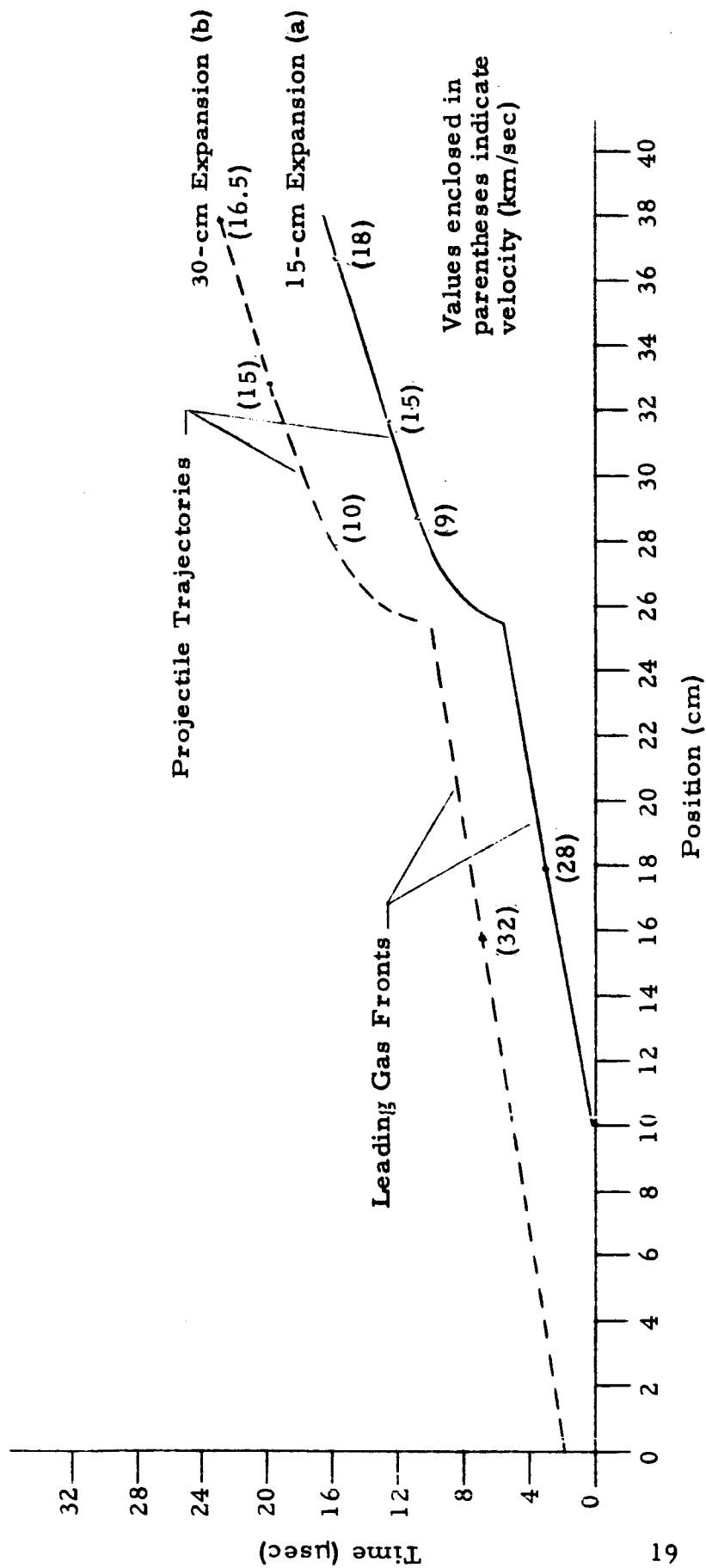
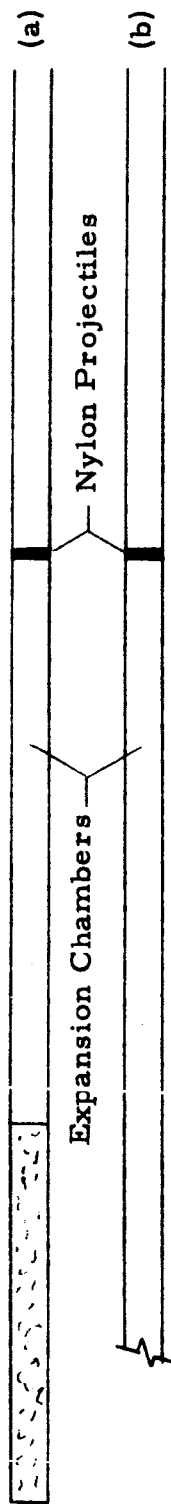


FIGURE 11. CALCULATED GAS KINETICS AND PROJECTILE ACCELERATION FOR TWO DIFFERENT LENGTHS OF EXPANSION CHAMBERS



model and a 50-cm expansion chamber, which resulted in a relatively slow (1.2 km/sec), but completely intact, projectile. In shots LP-1 and L-5 the expansion chamber was successively shortened to 30 cm and 15 cm, respectively. Shot L-5 accelerated an intact projectile to 4.15 km/sec. Figure 12 shows the kinetics of this shot, while Figure 13 is a radiograph of the same shot showing the nylon projectile in flight. In shot L-6, an attempt to reduce the length of the expansion chamber to 5 cm resulted in the vaporization of the projectile. Shot L-8 was then fired to determine the reproducibility of the previously successful shot L-5. When the repeated shot resulted in a broken projectile of substantially less velocity, it was concluded that fabrication and assembly tolerances should be reduced further than was previously thought necessary.

Three additional shots were designed to test different techniques of launching the projectiles. Shot L-9 was designed to provide a dynamic tamper by extending the high explosive down and around the barrel. This was to delay barrel expansion and maintain the axial acceleration of the gas after it left the conical section. The shot resulted in a projectile that was broken into many pieces.

Since many of the shots which had used the direct acceleration geometry had resulted in vaporization of the plastic projectiles, shot S-5 was designed to make use of this phenomenon by placing small sapphire spheres on the surface of a plastic projectile and attempting to accelerate the spheres by the aerodynamic drag of the high-density vapor passing around the projectile. The pin diagnostics showed velocities on the order of 8.95 km/sec; however, the sapphire spheres were not resolved in the color framing camera record, except for the impact flash which occurred as they struck the aluminum target.

The barrel geometry of shot L-10 used an expansion chamber with a cross-sectional area that was four times the bore area of the standard barrel. This allowed the pressure pulse in the gas to be attenuated and

## Initial Configuration

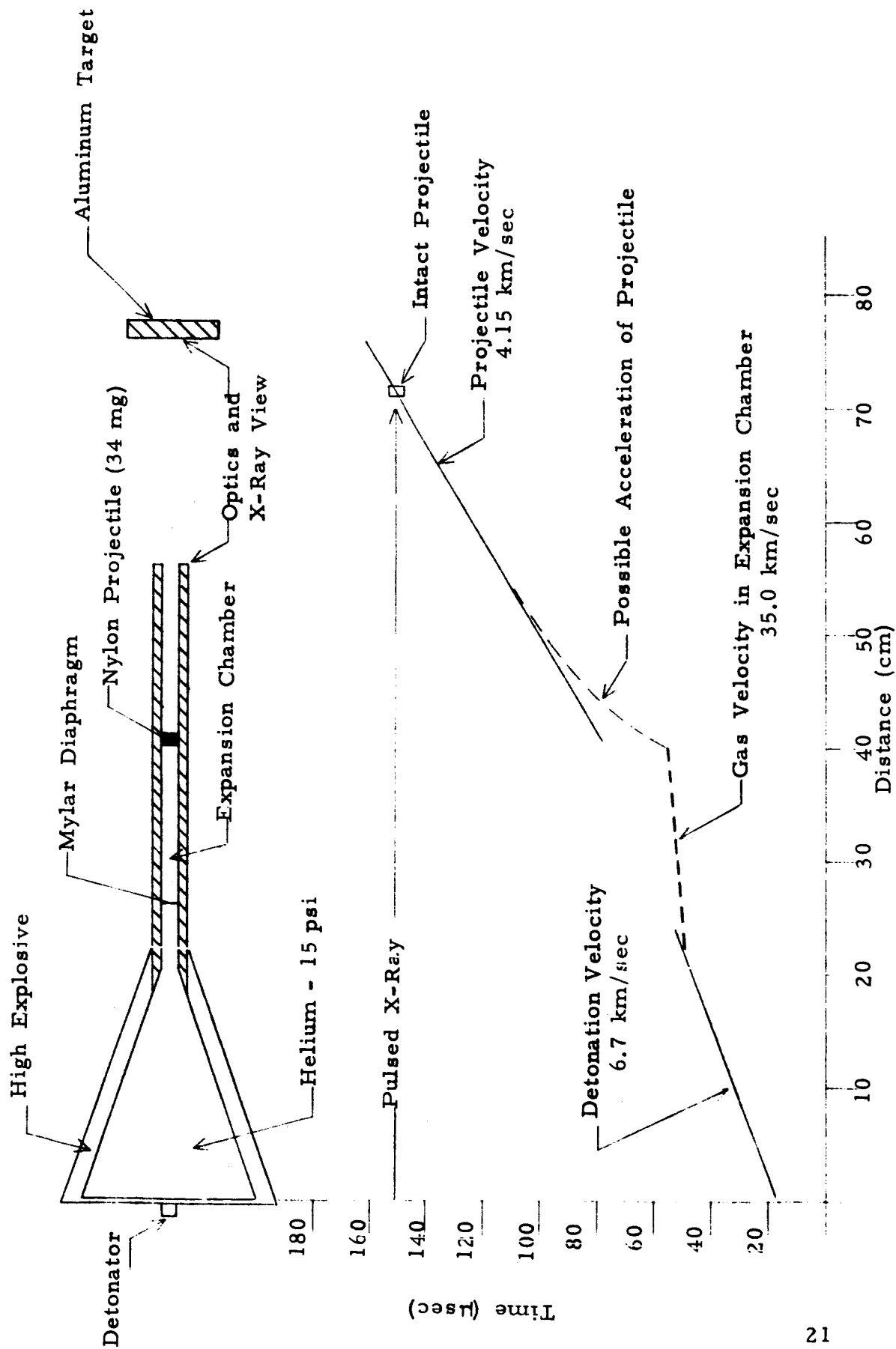


FIGURE 12. EXPERIMENTAL DATA OBTAINED FROM SHOT L-5

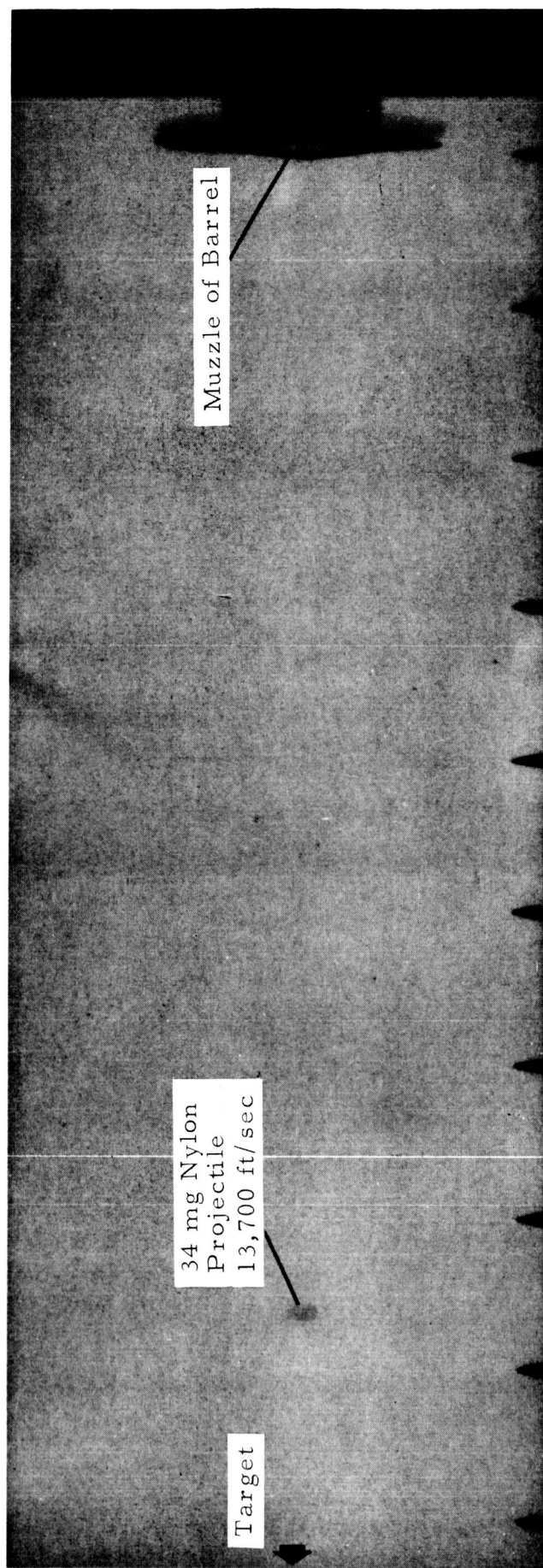


FIGURE 13. RADIOGRAPH OF PROJECTILE IN FLIGHT, SHOT L-5

broadened before encountering the projectile. In the linear hypervelocity gun this concept had proved highly successful by providing a reservoir of relatively low-pressure gas for projectile acceleration. The condition of the reservoir after the shot indicated high performance of the conical gun, but the projectile had been destroyed during the launching.

### III. LINEAR HYPERVELOCITY GUN

#### Theory and Analysis of Operation

The operation of the explosively driven linear hypervelocity gun is shown schematically in Figure 14. When the high explosive is detonated, the detonation front propagates along a cylindrical metal pressure tube containing a light gas. The resulting pressure collapses the tube, forming a conical-shaped region which functions much as a piston (Figure 14b). The motion of the piston drives a shock wave into the column of light gas which accelerates the gas to the detonation velocity of the high explosive. This velocity ranges between 5.0 km/sec and 8.8 km/sec, depending on the type of explosive used. The conservation of momentum across the shock front gives the pressure  $P_2$  in the shocked gas,

$$P_2 = P_1 + \rho_1 U S$$

in terms of the gas velocity  $U$ , the shock velocity  $S$ , and the initial gas density  $\rho_1$ . For the magnitude of pressures  $P_2$  being considered, the pressure  $P_1$  in front of the shock wave is negligible. Also, after the collapse of the tube becomes a steady-state process, the gas velocity is identical to the detonation velocity  $D$ . The above expression now becomes

$$P_2 = \rho_1 D S$$

Conservation of mass across the shock front yields

$$S = \frac{\rho_2 / \rho_1}{\rho_2 / \rho_1 - 1} D \qquad S = \frac{\eta}{\eta - 1} D$$

where the ratio of the density behind the shock wave  $\rho_2$  to the density in front of the shock wave  $\rho_1$  is defined as the compression  $\eta$ . By assuming the light gas is perfect, the maximum compression for a single strong shock

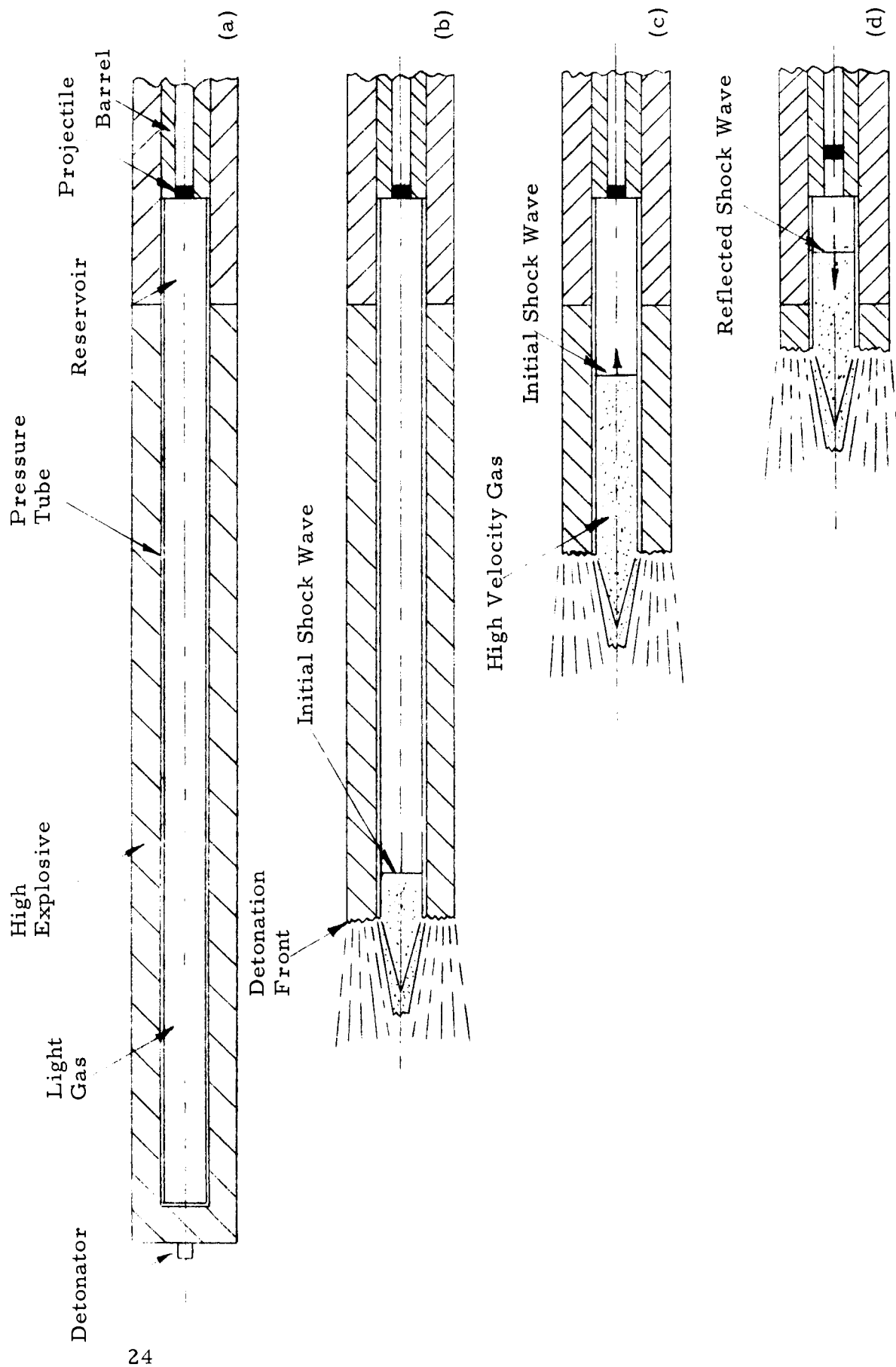


FIGURE 14. OPERATION OF THE LINEAR HYPERVELOCITY GUN

can be expressed in terms of the ratio of specific heats of the gas:

$$\eta = \frac{\gamma + 1}{\gamma - 1}$$

which yields

$$S = \frac{\gamma + 1}{2} D$$

for the shock velocity and

$$P_2 = \rho_1 \frac{\gamma + 1}{2} D^2$$

for the pressure behind the shock wave. The versatility of the linear gun is demonstrated by this pressure equation. The pressure in the light gas can be controlled over a wide range of gases ( $\gamma$ ), loading densities ( $\rho_1$ ), and high explosives (D).

The capabilities of the linear gun have been investigated most extensively in the geometry shown in Figure 14. The projectile is accelerated by using the pressure profile in the reservoir resulting from the reflection of the initial shock wave from a 4/1 area discontinuity between the pressure tube and barrel (Figure 14d). Assuming both a perfect gas and reflection from a rigid wall, the pressure behind the reflected shock wave  $P_3$  would be

$$P_3 = \frac{3\gamma - 1}{\gamma - 1} P_1$$

The thick steel walls of the reservoir section delay appreciable two-dimensional effects, such as rarefactions, resulting from the expansion of this region, until the projectile has been accelerated. This makes the acceleration process of the linear gun more amenable to one-dimensional calculations and analysis than the corresponding process in the conical gun.

Physics International's 1-1/2-dimensional hydrodynamics code (DOAH) has been used to calculate the acceleration of projectiles and has proved invaluable for parametric studies and design improvements. This code is basically a one-dimensional, time-dependent, Lagrangian

hydrodynamic code that treats cross-sectional area changes along the single dimension as a separate subroutine. Radial wall motion, radiation losses, and extraction and addition of mass are other space-time phenomena which are treated as subroutines of the one-dimensional code. Figure 15 gives calculations of this type, showing the dynamics of accelerating a polyethylene projectile by the pressure profile of a perfect gas ( $\gamma = 5/3$ ) which has been shocked to an initial pressure of 4.0 kb by the motion of a hypothetical piston moving at 6.2 km/sec. The initial shock is reflected from an area ratio of 9/1. Figure 16 presents the pressure profile at the base of the projectile.

### Experimental Results

Table II summarizes the results of the twelve shots which have been fired using the linear hypervelocity gun. Two different high explosives have been investigated as energy sources for these guns: (1) a solid pertalnythnital tetranitrate mixture, EL-506C, which is supplied by E. I. Dupont de Nemours and Company in the form of flexible tubing (detonation velocity = 7.0 km/sec at a density = 1.48 gm/cm<sup>3</sup>) and (2) nitromethane which is sensitized by the addition of 3 percent ethylene diamine (detonation velocity = 6.2 km/sec at density = 1.13 gm/cm<sup>3</sup>). Shots CLG-1 through CLG-10 used the flexible solid explosive while the sensitized nitromethane was used for the remaining shots.

Prior to this program, the authors had used the linear gun to directly accelerate projectiles whose cross-sectional areas were the same as the pressure tube. These projectiles were accelerated to 4.55 km/sec using the pressure profile in the gas resulting primarily from the initial shock pressure  $P_1$  described in the previous section. Shot CLG-1 was the first linear gun design that utilized the pressure reservoir created by the reflection of the initial shock from the area discontinuity (a quasi-rigid wall). This design yields a sustained pressure profile that is less affected by the subsequent motion of the projectile. Shot CLG-1 accelerated an intact 0.156-gm nylon projectile to 6.7 km/sec. The light gas was helium with an initial loading pressure of 480 psi. The barrel was 4 in. long.

TABLE II. EXPERIMENTAL RESULTS OF EXPLOSIVELY DRIVEN LINEAR HYPERVELOCITY GUNS

Shot No.	Experiment	Explosive Weight (lb)	Explosive Type	Gas		Barrel		Projectile		Velocity		Projectile Condition	Remarks
				Type	Pressure (psi)	Diam. (in.)	Length (in.)	Diam. (in.)	Length (in.)	km/sec	ft/sec		
CLG-1	First reservoir gun	3.5	EL506C	helium	480	0.290	4	nylon	0.290	0.135	6.7	22,000	Excellent First linear gun using reservoir concept. Fired 3/26/65
CLG-2	Explosive extended around barrel	4.5	EL506C	helium	480	0.290	24	nylon	0.290	0.137	6.7	22,000	Unstable secondary acceleration. Fired 4/7/65
CLG-3	Hydrogen driver gas	3.5	EL506C	hydrogen	680	0.290	4	nylon	0.290	0.139	7.2	23,600	Fired 4/22/65
CLG-4	Higher loading pressure	3.5	EL506C	helium	960	0.255	6	nylon	0.255	0.137	6.6	21,600	Excellent projectile condition. Fired 5/13/65
CLG-5	Lower loading pressure	3.5	EL506C	helium	240	0.220	6	nylon	0.220	0.115	0.082	>21,600	Basalt impact: Velocity uncertain due to loss of camera record. Fired 6/11/65
CLG-6	Repeat CLG-5	3.5	EL506C	helium	240	0.214	6	nylon	0.220	0.113	0.078	21,600	Fired 6/17/65 Basalt impact
CLG-7	Repeat of CLG-1 plus modified taper	3.5	EL506C	helium	480	0.210	6	nylon	0.215	0.116	0.076	22,150	Fired 6/17/65 Diatomaceous Earth Impact
CLG-8	High-density polyethylene projectile	3.5	EL506C	helium	480	0.212	6	HDPE	0.224	0.115	0.066	26,200	Fired 6/29/65
CLG-9	Repeat CLG-4 except evacuated	3.5	EL506C	helium	960	0.212	6	nylon	0.220	0.115	0.083	26,200	Fired 6/30/65
CLG-10	Leaky piston	3.5	EL506C	helium	2300	0.212	12	nylon	0.220	0.116	0.079	>3.8	Good Crater showed evidence of steel fragments. Fired 7/7/65
IR-1	Infinite reservoir	6.5	NM+EDA	helium	645	0.217	12	HDPE	0.249	0.115	0.082	>0.60	Radial pressure gradients possibly broke projectile Fired 6/21/65
SP-1	Accelerated reservoir	6.5	NM+EDA	helium	645 220	0.255	8.5	nylon	0.265	0.161	0.10	28,200	Best velocity obtained with linear gun Fired 7/15/65
CLEG-1	Expansion chamber	3.0	NM+EDA	helium	1200	0.208	9.0	nylon	0.214	0.105	0.070	18,800	Broke in flight Fired 7/28/65



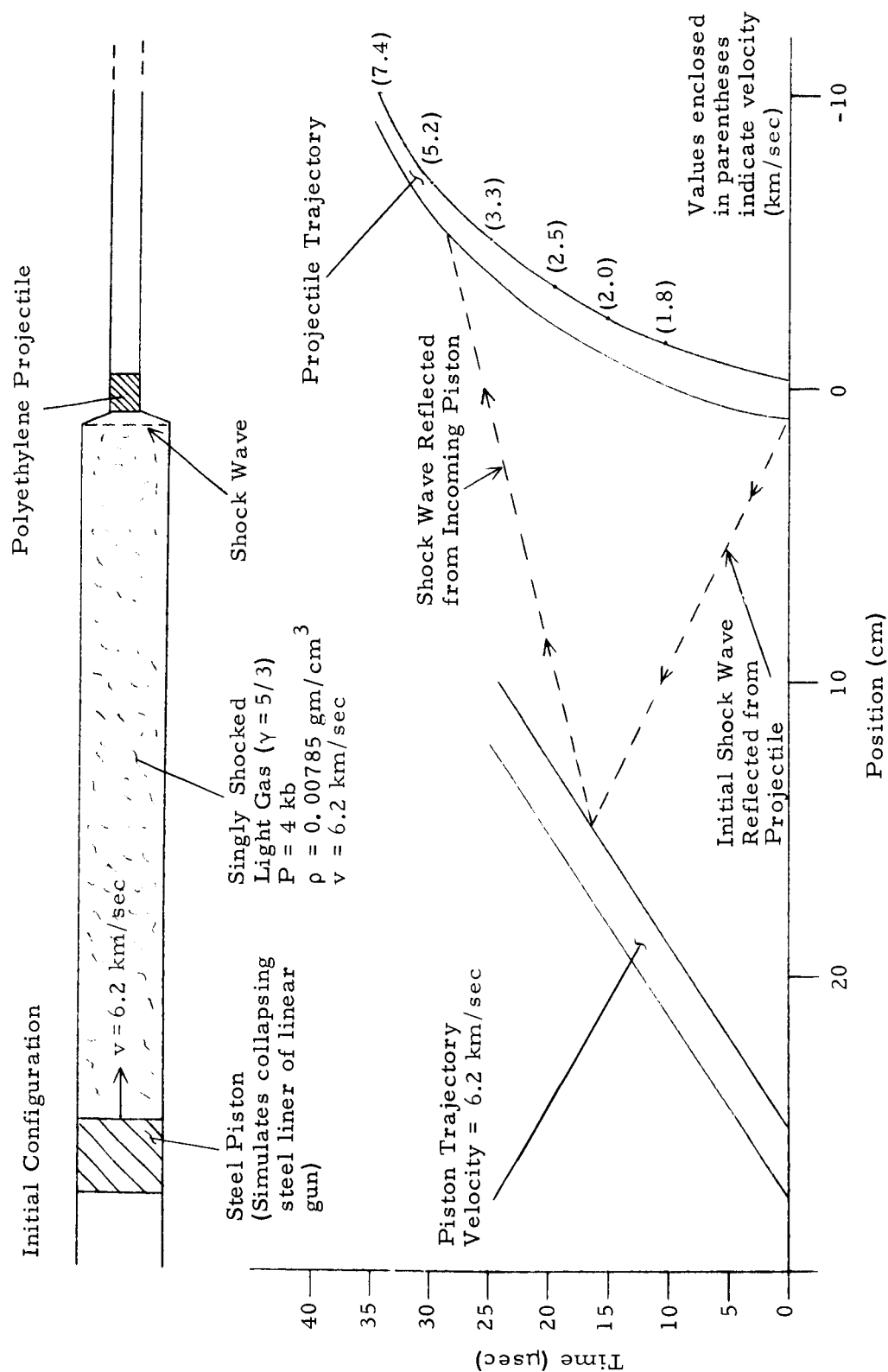


FIGURE 15. CALCULATED OPERATION OF LINEAR RESERVOIR GUN

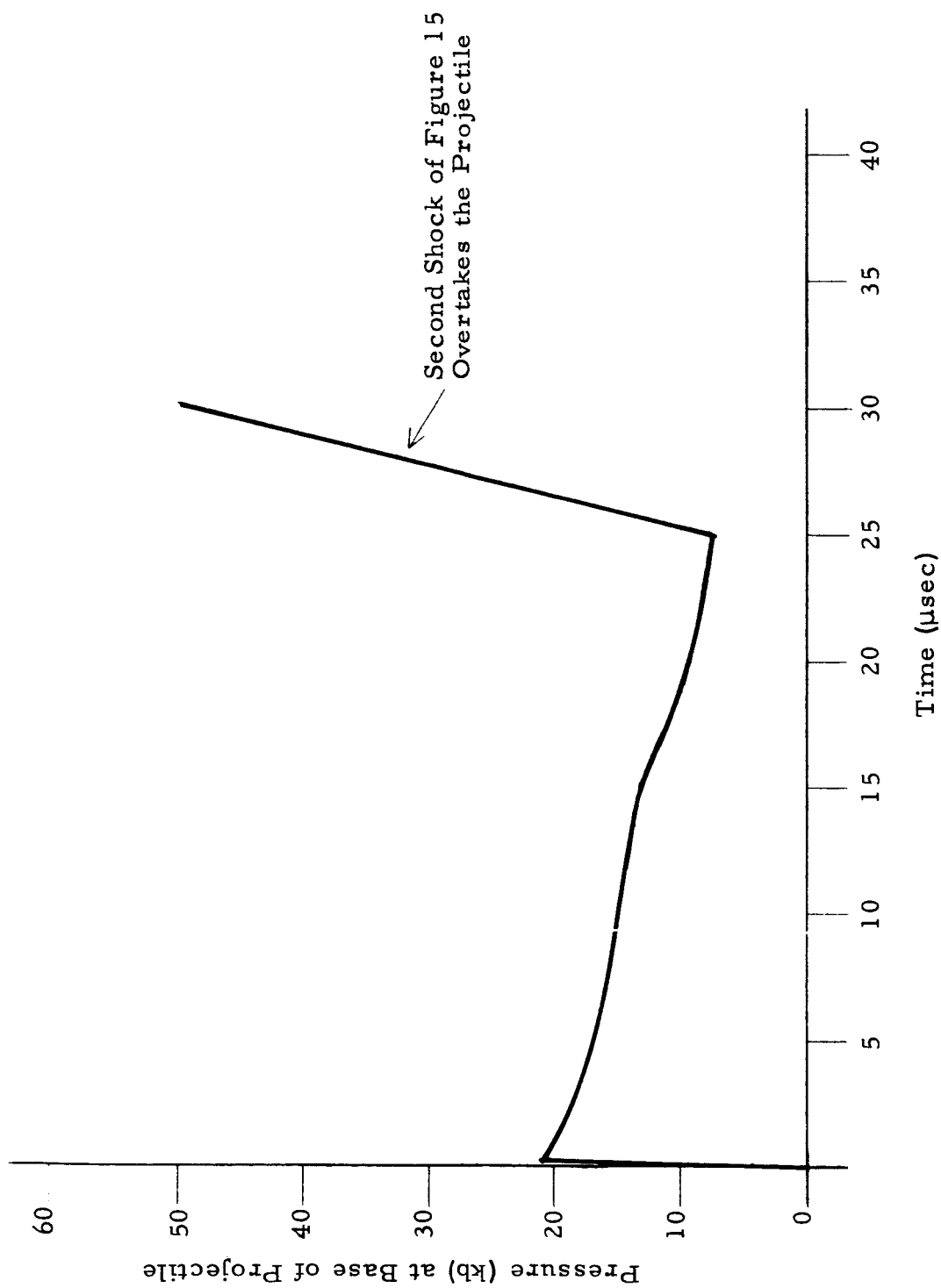


FIGURE 16. CALCULATED BASE PRESSURE DURING ACCELERATION OF POLYETHYLENE PROJECTILE BY A LINEAR RESERVOIR GUN

The pressure behind the initial shock wave was 4 kb which, reflected, produced a reservoir pressure of approximately 20 kb.

For the next shot (CLG-2), additional high explosive was placed around an extended thin-walled barrel which was employed to provide a secondary acceleration by collapsing the barrel behind the already moving projectile (Figure 17). The high-speed framing camera showed the projectile was broken into two pieces moving at 6.7 km/sec. It was concluded that enough gas could not have been trapped behind the moving projectile to properly support a secondary acceleration.

In shot CLG-3, hydrogen replaced the helium as a driver gas. The initial loading pressure of the hydrogen was adjusted to give a 4-kb pressure behind the initial shock wave by assuming an average ratio of specific heats ( $\gamma$ ) for the expected temperature range. The projectile was accelerated to 7.2 km/sec and seemed intact on the framing camera record. However, the crater produced in a 6061-T6 aluminum target indicated that there may have been a small fracture or extrusion of the projectile.

In order to determine the range of pressures in which the reservoir design would operate without breaking the projectile, three shots were fired in which the helium loading pressures were 960 psi (CLG-4) and 240 psi (CLG-5 and a repeat shot CLG-6), corresponding to pressures behind the initial shock wave of 8 kb and 2 kb, respectively. The 0.133-gm nylon projectile using the 8-kb initial shock pressure was accelerated to 6.7 km/sec and remained intact. The condition of the pellet was determined by a pulsed radiograph, color framing-camera sequence, and the smooth hemispherical appearance of the crater produced in 6061-T6 aluminum. The 2.0-kb initial shock pressure accelerated a broken projectile to a velocity of 6.7 cm/sec. The dynamics of these shots are shown in Figures 18 and 19. The experimental data presented in these

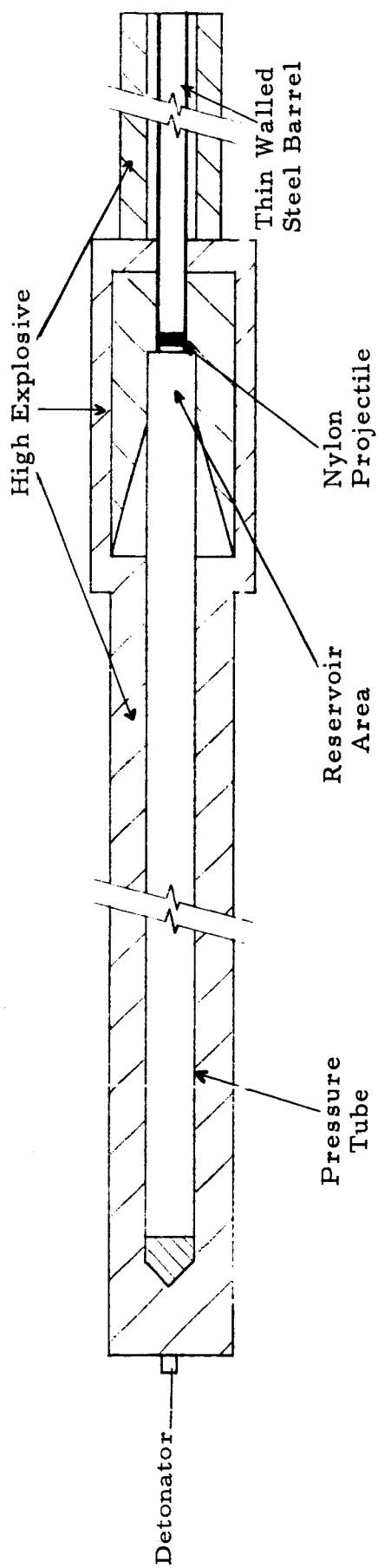


FIGURE 17. SHOT CLG-2

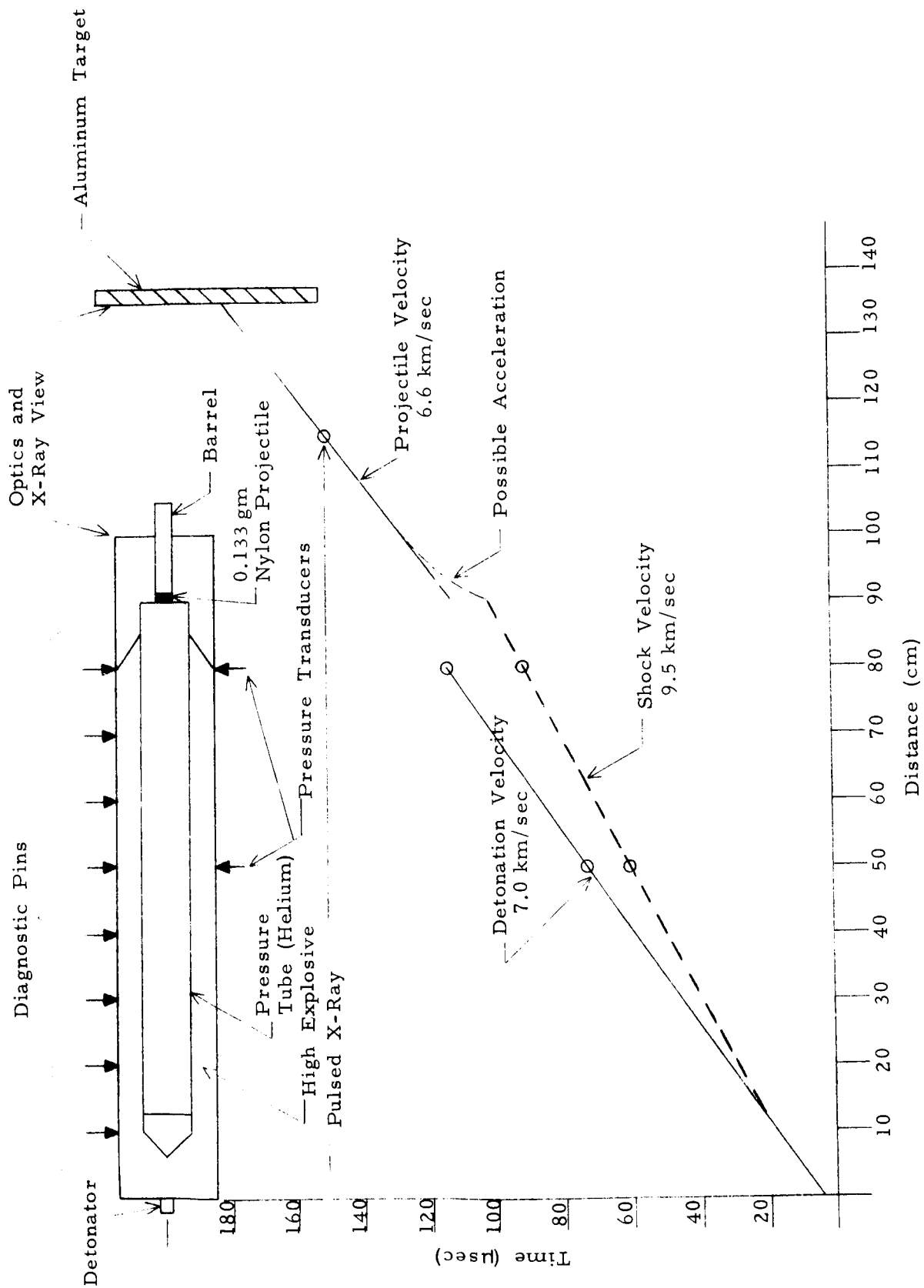


FIGURE 18. EXPERIMENTAL RESULTS OF SHOT CLG-4

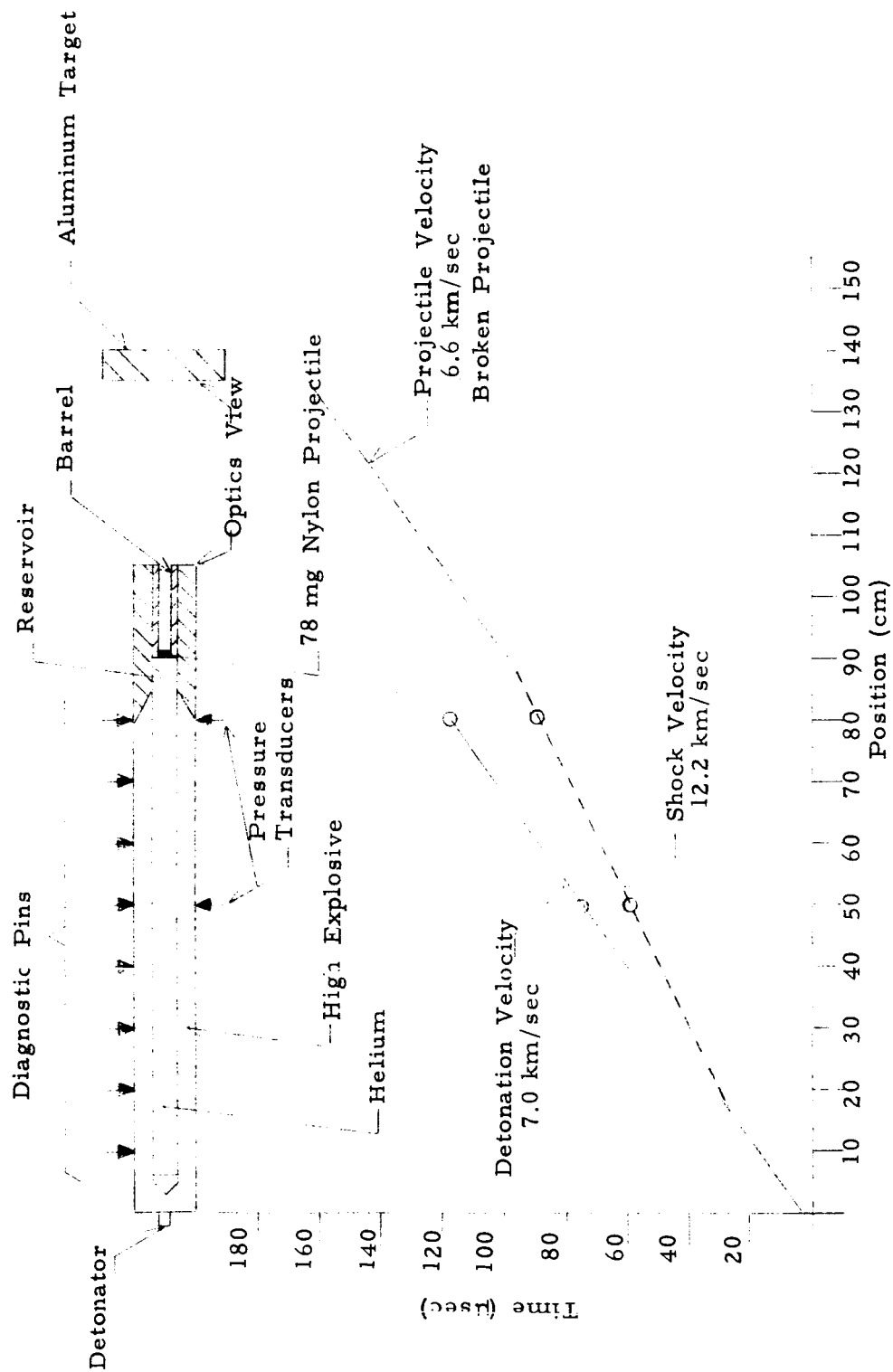


FIGURE 19. EXPERIMENTAL RESULTS OF SHOT CLG-6

figures were obtained from monitoring the shock velocity in the pressure tube, the detonation velocity of the high explosive, and the projectile velocity. The shock velocity of shot CLG-4 (960 psi helium loading pressure), was found to be 9.5 km/sec. Previous shots, with 480 psi loading pressure, had exhibited the same shock velocity. This velocity agrees quite well with the theoretical value of 9.3 km/sec obtained from the conservation of mass across a shock wave for an ideal gas, moving at 7.0 km/sec, whose ratio of specific heats is 5/3:

$$S = \frac{\gamma + 1}{2} D \quad D = 7.0 \text{ km/sec} \quad \gamma = 5/3 \rightarrow S = 9.3 \text{ km/sec}$$

However, the shock velocity observed for the shot with the lower loading pressure (CLG-6) was found to be 12.2 km/sec. It was postulated that the lower pressures produced behind the initial shock permitted surface or metal gases in the pressure tube to be driven out ahead of the collapsing tube. This would create a pseudo-piston with a velocity greater than that of the collapsing tube, which would then drive the shock wave at a higher velocity.

Polyethylene was used as the projectile material in shot CLG-8, replacing the previously used nylon. The observed velocity of 8.0 km/sec was expected with the change in projectile density. For a given length of projectile, high-density polyethylene (density = 0.92 gm/cm<sup>3</sup>) presents a smaller areal density than does nylon (density = 1.12 gm/cm<sup>3</sup>). However, the projectile was broken into several pieces.

To determine the effect of increasing the area ratio between the reservoir and barrel, a ratio of 36 was used in shot IR-1 instead of the ratio of 4 previously used. This gun required sensitized nitromethane since the flexible tube explosive was not available in the larger diameters. The larger driver section, explosive, and pressure tube needed for this experiment had been developed in the process of scaling-up a linear hypervelocity gun to accelerate 5-lb projectiles to 6 km/sec under ARPA contract DA 04-200-AMC-796(X). The aim

was to provide an "infinite reservoir" for the acceleration of the projectile; however, the projectile was completely destroyed during launching. The cause of the breakup is not clear. The large area at the end of the "infinite reservoir" results in a strong plane shock propagating down the steel barrel. This shock may create radial pressure gradients in the projectile sufficiently strong to break it up.

In the first four shots, CLG-1, -2, -3, and -4, the light gases had been introduced into the pressure tube without first evacuating the existing atmosphere of air. This meant that, for a helium loading pressure of 480 psi, 22.4 percent by weight of the gas was composed of air molecules. The pressure tubes of subsequent shots were evacuated to obtain pure helium. It was obvious that projectile integrity had generally deteriorated in these latter shots. Shots CLG-7 and CLG-9 were fired to repeat, respectively, shots CLG-1 and CLG-4 (which had launched projectiles in excellent condition), with the exception that the pressure tubes were evacuated prior to introducing the helium. Both repeat shots showed some degree of projectile breakup, indicating that the helium-air mixture provides a certain degree of pressure or temperature attenuation.

To realize the full potential of a projector using the reservoir principal, a constant pressure is necessary at the base of the projectile. Since the initial motion of the projectile rapidly decreases this pressure, a constant base pressure can be attained only by a gradually increasing pressure in the reservoir. Three prototype shots, designed to create a rising pressure profile, have been fired.

Shot CLG-10 used a small steel piston positioned in front of the reservoir with three off-axis orifices whose cross-sectional area was



1/10 that of the piston (a "leaky piston"). Diaphragms were placed over the orifices. The principal of operation requires that, as the initial shock proceeds into the reservoir, it ruptures the diaphragms, allowing gas to leak into the reservoir. The piston is then set in motion by the initial and reflected shocks, and continues to compress the gas in the reservoir. The projectile was accelerated to approximately 3.8 km/sec, but the relatively low velocity pre-empted the optical and radiographic diagnostics used to determine projectile condition. The impact on a 6061-T6 aluminum target showed a primary crater which seemed to have been formed by the projectile, and a secondary crater imbedded by a steel fragment, which is believed to have been part of the leaky piston. This "leaky piston" design shows much promise for providing a rising pressure profile, and is discussed more fully in the Appendix. Considerably more theoretical and experimental work will be required to realize the potential of this design.

Another technique of tailoring the pressure profile is by introducing an evacuated region (expansion chamber) between the light gas and projectile, allowing the pressure pulse to attenuate and lengthen before encountering the projectile. Shot CLEG-1 used a 0.020-in. stainless steel diaphragm located 24 in. in front of the projectile, forming an expansion chamber. The projectile was accelerated intact to 5.73 km/sec, but broke up in flight.

The accelerated reservoir concept used in standard light-gas guns was also investigated as a means for producing a constant pressure at the base of the projectile. Figure 20 shows the calculated position-time and base-pressure-time histories resulting from simulating the accelerated reservoir concept on the Physics International 1-1/2 dimensional hydrodynamic computer code (DOAH). This calculation used a high-density polyethylene piston with an areal density of  $1.17 \text{ gm/cm}^2$  to shock-heat and accelerate a light gas ( $\gamma = 5/3$ ) in a tapered reservoir whose cross-sectional area changed by a factor of 9 over a distance of 15.0 cm. A high-density polyethylene projectile with an areal density of  $0.37 \text{ gm/cm}^2$  was located in the breech of the tapered barrel. The pressure profile at

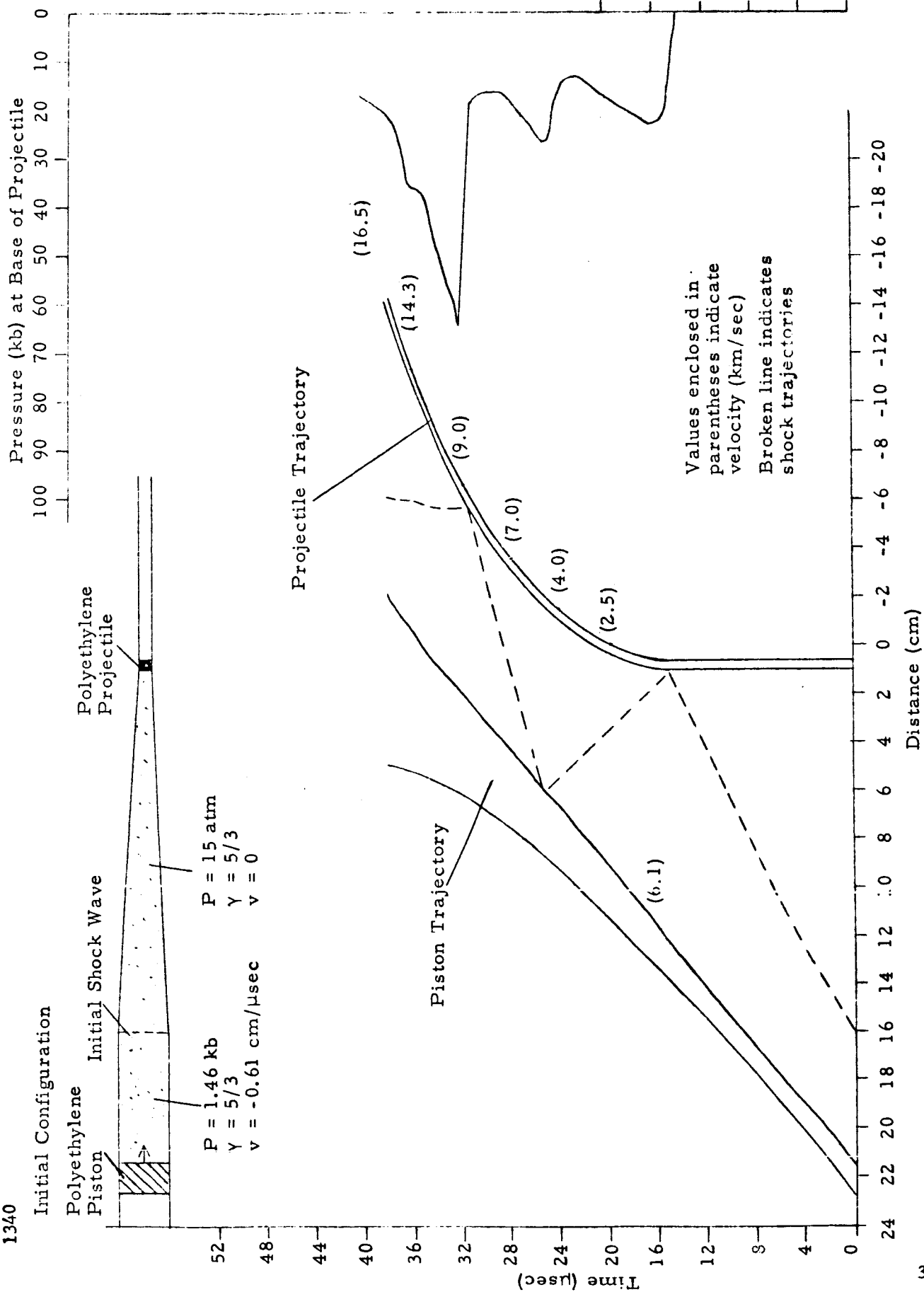


FIGURE 20. CALCULATED POSITION-TIME AND BASE-PRESSURE-TIME HISTORIES OF AN ACCELERATED RESERVOIR HYPERVELOCITY PROJECTOR USING A 15-cm TAPERED RESERVOIR

the base of the projectile (Figure 20b) remained quite constant during the acceleration process, resulting in a projectile velocity of 16.5 km/sec before the calculation was terminated.

Shot SP-1 was designed and fired on the basis of this calculation. The nylon projectile was broken during acceleration; however, the fragments were observed to have the highest velocity of the linear gun experiments (8.6 km/sec). During fabrication of the shot, a prohibitive delay in obtaining a specially ground tapered reamer required that the tapered section be shortened to 7.5 cm. The effect of this change is demonstrated in the results of a computer calculation (Figure 21) which simulated shot SP-1 as it was fired. Here one sees that the shock wave which is initially reflected from the projectile is again reflected a short time later from the incoming piston. When this shock reaches the projectile, it subjects the projectile to an impulsive peak pressure of 175 kb. This pressure was probably responsible for the projectile breakup.

#### IV. DIAGNOSTIC TECHNIQUES

The hypervelocity guns are assembled complete with their flight range and attached instrumentation in a special preparation room while the containment vessel and external instrumentation are being readied for firing. Figures 22 and 23 are set-up photographs taken of conical shot S-2 and linear shot CLG-4 prior to firing. The diagnostic instrumentation can be divided into three general categories: (1) operation of the explosively driven projector, (2) kinetics of the driven gas before it encounters the projectile and as it encounters the projectile, and (3) analysis of the accelerated material.

##### Operation of the Projectors

The detonation of the high explosives and the movement of

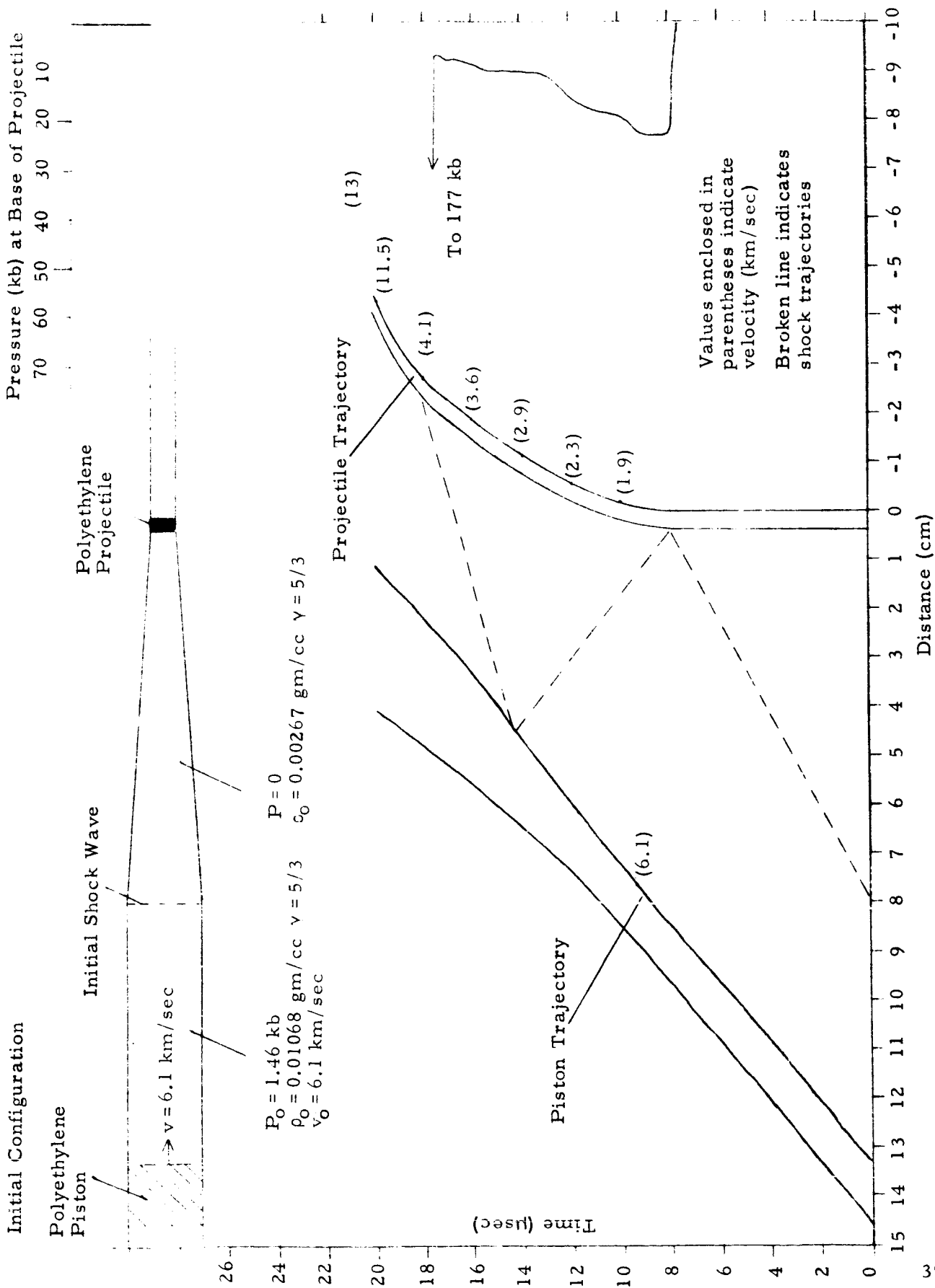


FIGURE 21. CALCULATION SIMULATING SHOT SP-1 AS FIRED WITH 7.5-cm TAPERED RESERVOIR

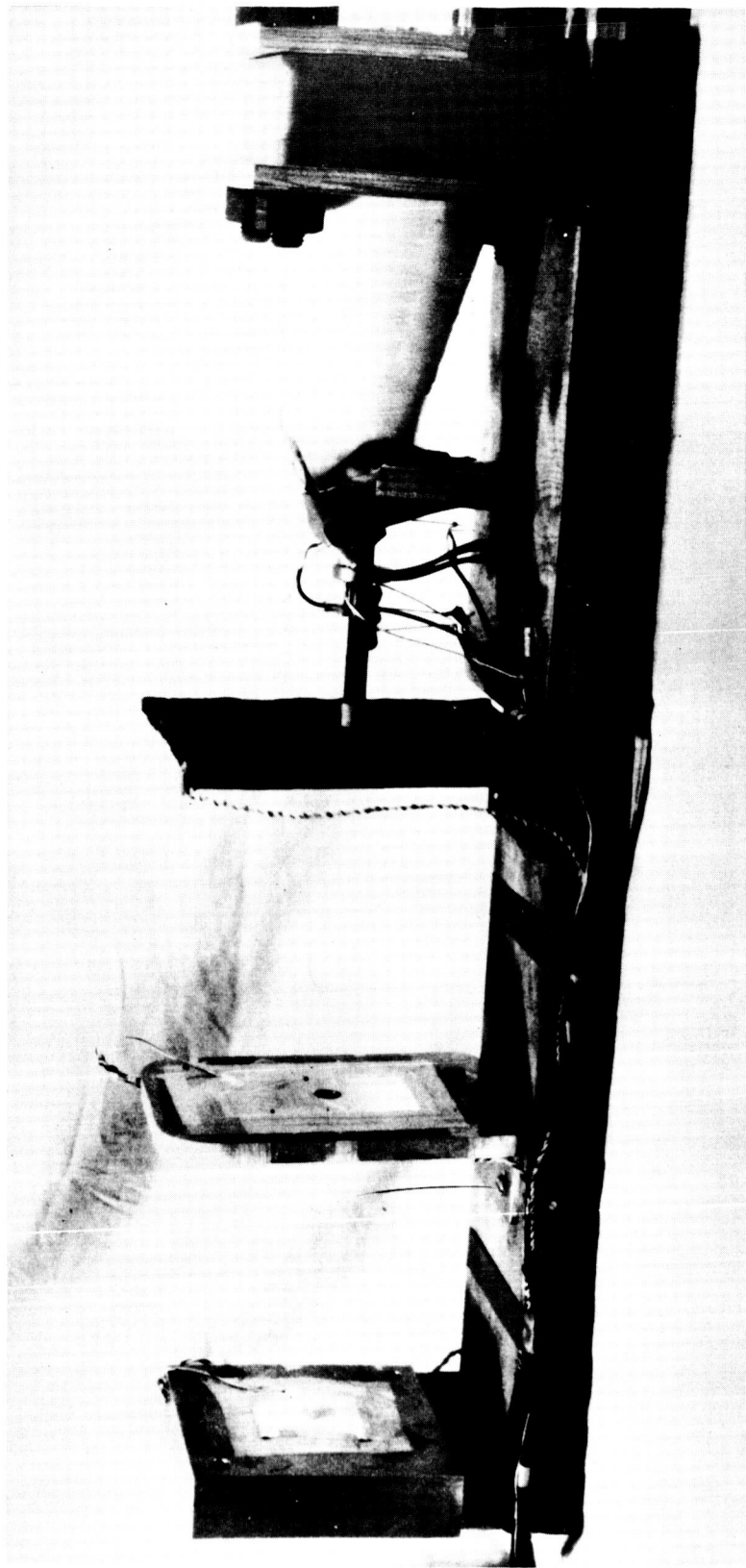


FIGURE 22. HYPERVELOCITY GUN ASSEMBLY FOR CONICAL SHOT S-2

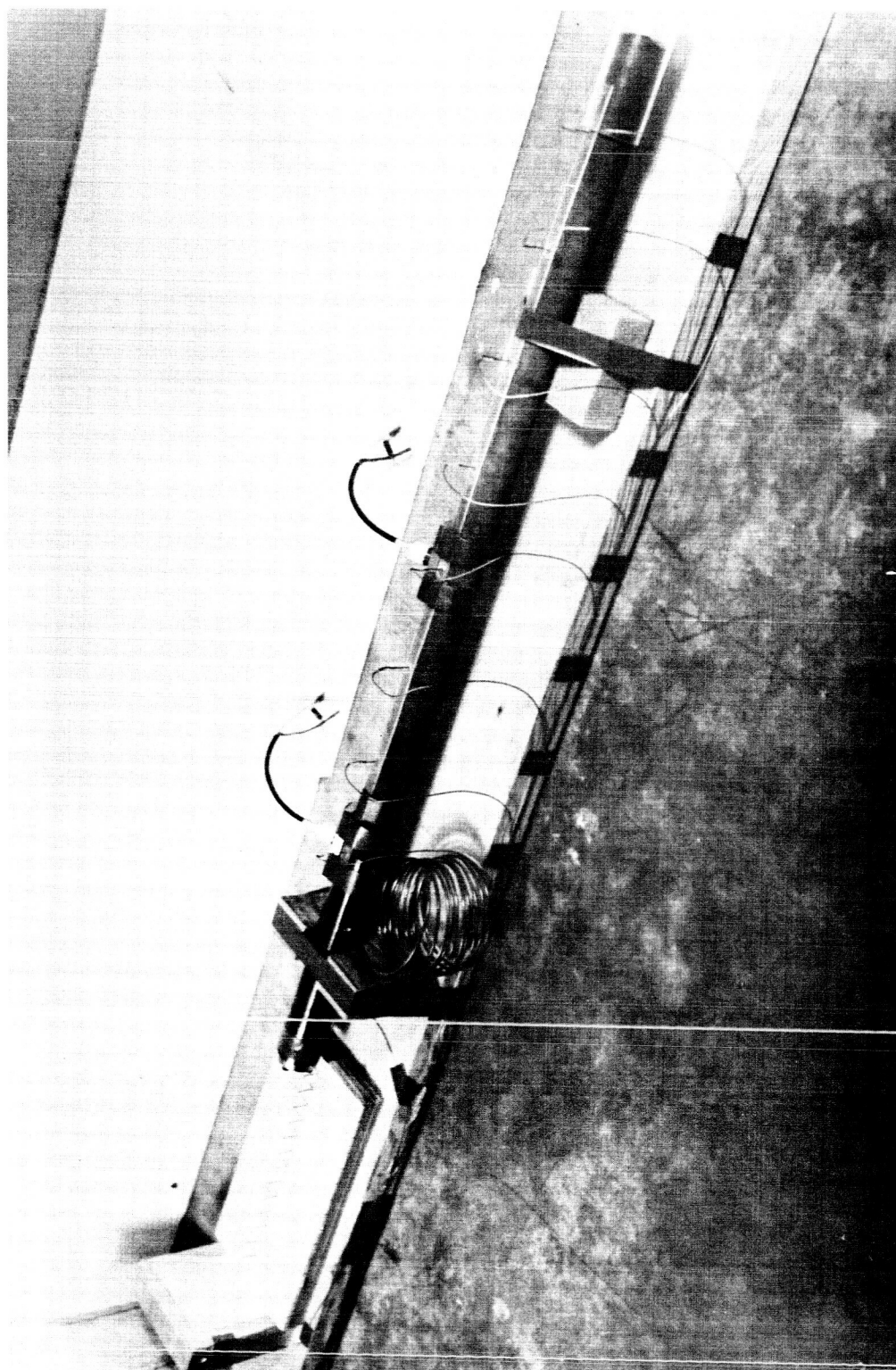


FIGURE 23. HYPERVELOCITY GUN ASSEMBLY FOR LINEAR SHOT CLG-4

explosively driven metal liners is measured with commercially available, capped, shorting pins obtained from Edgerton, Germeshausen, and Grier, Inc. These pins are coaxial, with a 0.032-in. body and a 0.002-in. shorting gap. Figure 24 is a drawing of the pins with a graph of their operational characteristics, provided by the manufacturer. The pin senses the arrival of the pressure front and provides a switch closure to trigger a pulse discharge. The pulses are recorded on raster-type oscilloscopes which have a total recording time of  $115 \mu\text{sec}$ , fiducial markers every  $0.5 \mu\text{sec}$ , and a time resolution of  $0.05 \mu\text{sec}$ . The pulses are coded for polarity, length, and height. A typical pulse length is  $0.1 \mu\text{sec}$ . A back-up record of 8 pin signals is shown on the upper trace of Figure 28.

The detonation of the high explosives is also measured by phototransistors that record the passage of the highly luminous detonation front past narrow collimating slits. Figure 25 shows a typical record. There is a sharp rise as the luminous front enters the slit aperture, a flat top at the saturation of the phototransistor, and a return to the base line as the detonation passes out of view.

Radiographs of the gun's operation are taken with a high-intensity, medium-energy, portable X-ray system. A Marx-type generator, designed and built by Physics International, drives a remotely located flash X-ray tube (Field Emission Corporation Model 506A). The output is a square wave of  $0.2 \mu\text{sec}$  duration in the energy range of 300 to 600 kV. Figures 4 and 5 are sample radiographs taken of the conical gun liner during its implosion. Another diagnostic example of gun operation is shown in Figure 26. This radiograph shows the collapse of the pressure tube of linear shot CLG-9. The upper radiograph gives the final setup before firing, showing the pressure tube entering the reservoir. The lower radiograph was taken at the time the shock front reached the projectile, and shows the pressure tube ahead of the detonation, expanded by the shocked gas, and the implosion of this tube

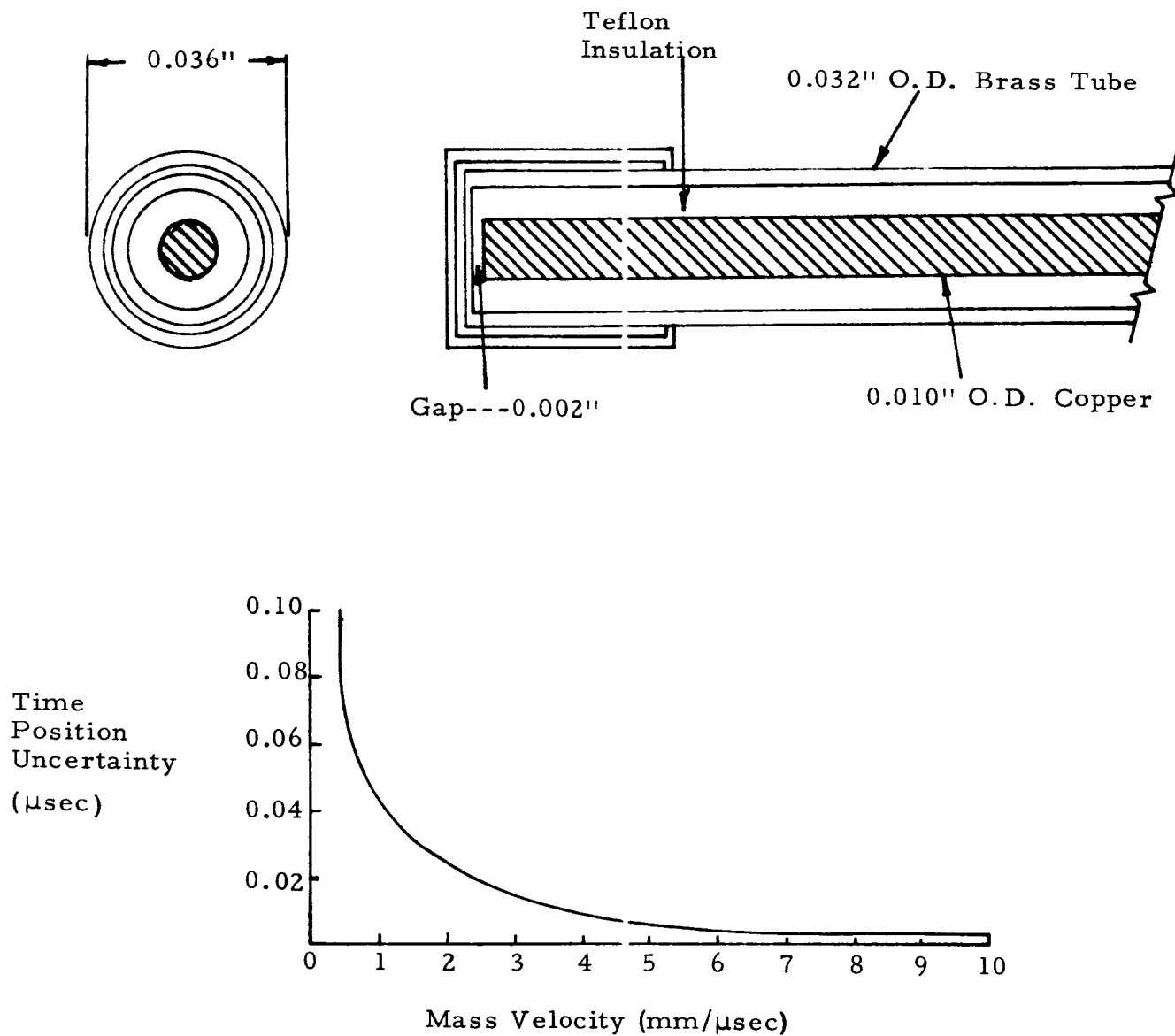


FIGURE 24. 0.032-INCH COAXIAL SELF-SHORTING PIN, SCHEMATIC AND OPERATIONAL CHARACTERISTICS



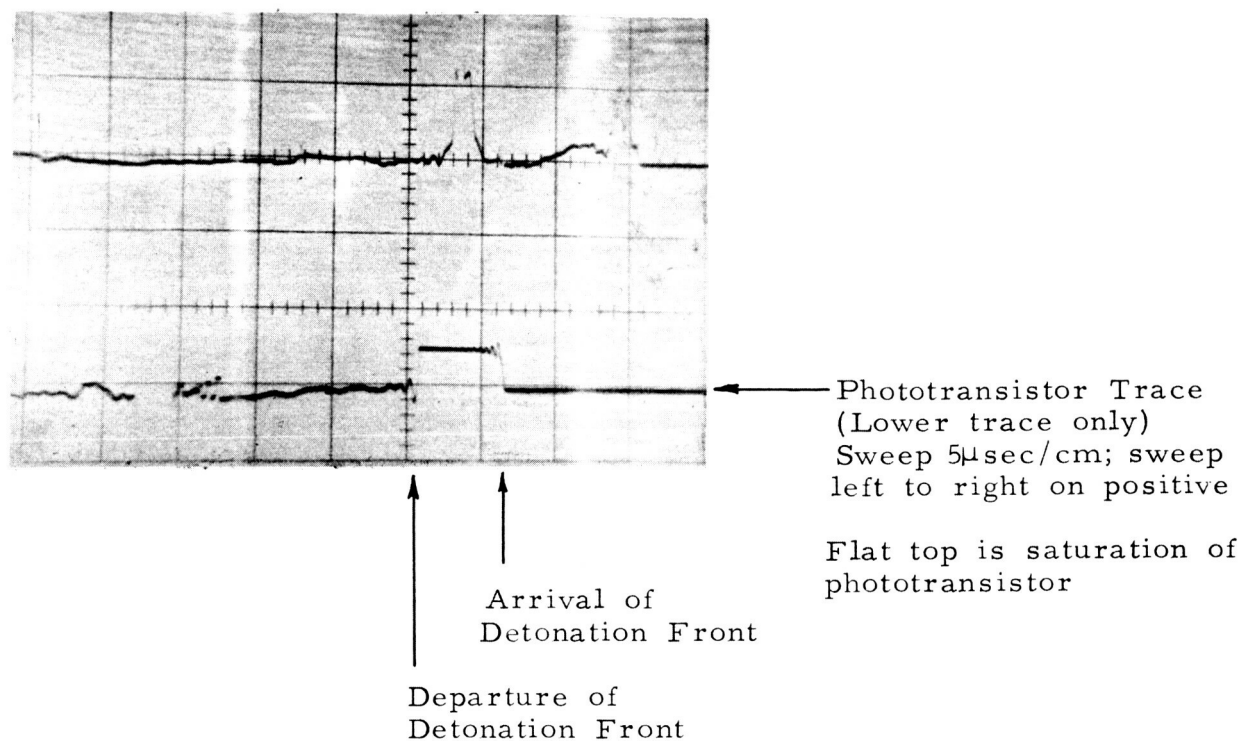


FIGURE 25. TYPICAL PHOTOTRANSISTOR TRACE (SHOT CLG-8)

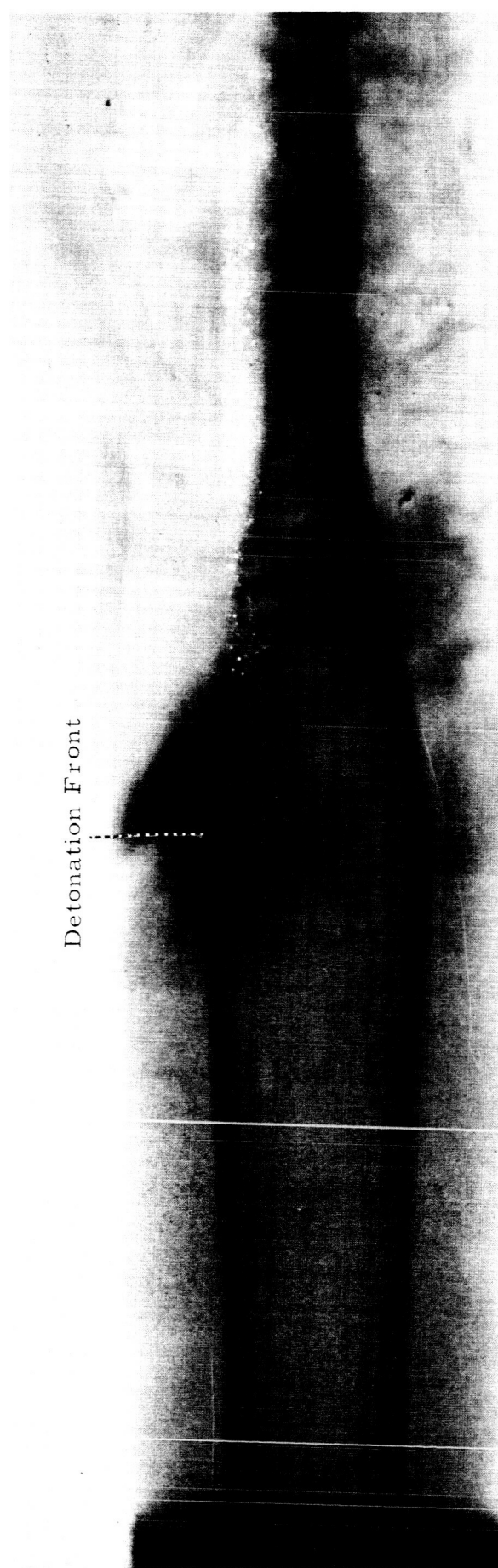
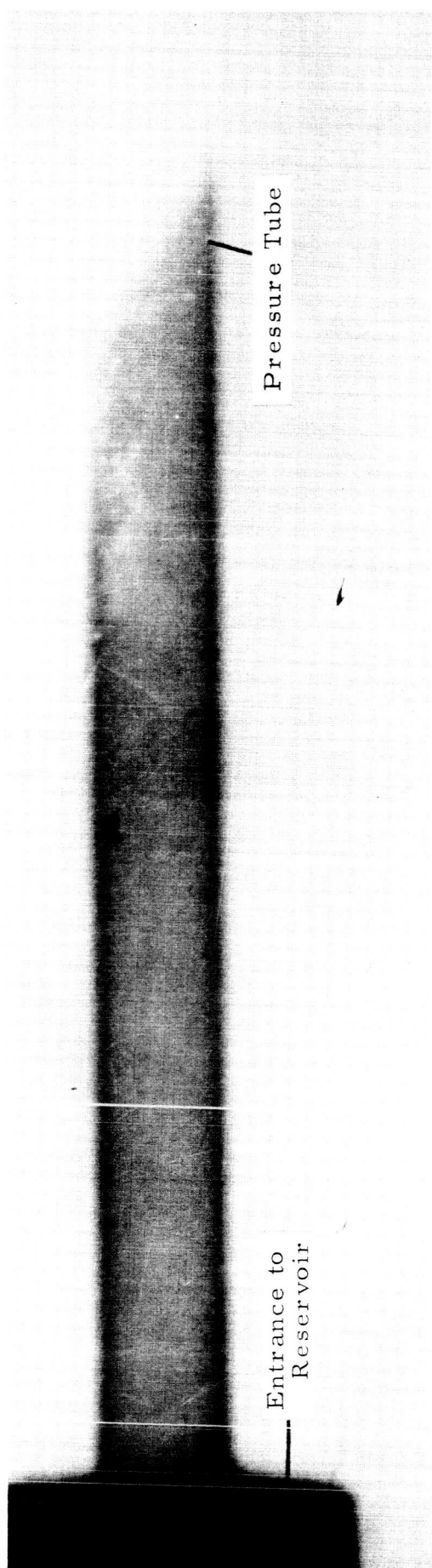


FIGURE 26. SETUP AND SHOT RADIOGRAPHS OF SHOT CLG-9

behind the same detonation front. This X-ray system is also used to check the gun assemblies prior to firing, as in Figure 26a and Figure 27, which is a radiograph of conical shot S-3 taken during the final setup run. The Marx generator stands 4 ft tall, is 2-1/2 ft in diameter, and weighs approximately 1200 lb, permitting it to be readily transported where needed.

### Kinetics of the Gas

The velocity of the shock front in the driver section and pressure reservoir is measured with special barium-titanate piezoelectric pressure transducers developed and constructed by Physics International to fit standard UHF coaxial connector cables. Once the transit time of the shock wave through the intervening material has been measured with two such transducers, these units can be placed outside the high explosives or steel containers and read back to give precise measurement of the position-time history of the shock front inside the gun, as well as that of the detonation front. The output of these transducers is 1.1 amp/kb. The lower trace of Figure 28 is a record of a transducer placed on the high explosive of linear shot CLG-6, showing the passage of the initial shock wave, the reflected shock wave, and the arrival of the detonation.

The movement of the shock front through the expansion chamber and barrel is measured with uncapped shorting pins inserted in the wall and open to the bore. They operate as ionization sensors, completing a pulse circuit in the same manner as the capped pins. These pins were also placed in the barrel to record the acceleration of the projectile. They were very effective in providing the time at which the projectile started moving (and therefore the average acceleration), but succeeding pins located in the bore of the barrel were pre-triggered by gases moving around and ahead of the projectile.

### Analysis of Accelerated Material

All guns are provided with an ionization switch on the muzzle

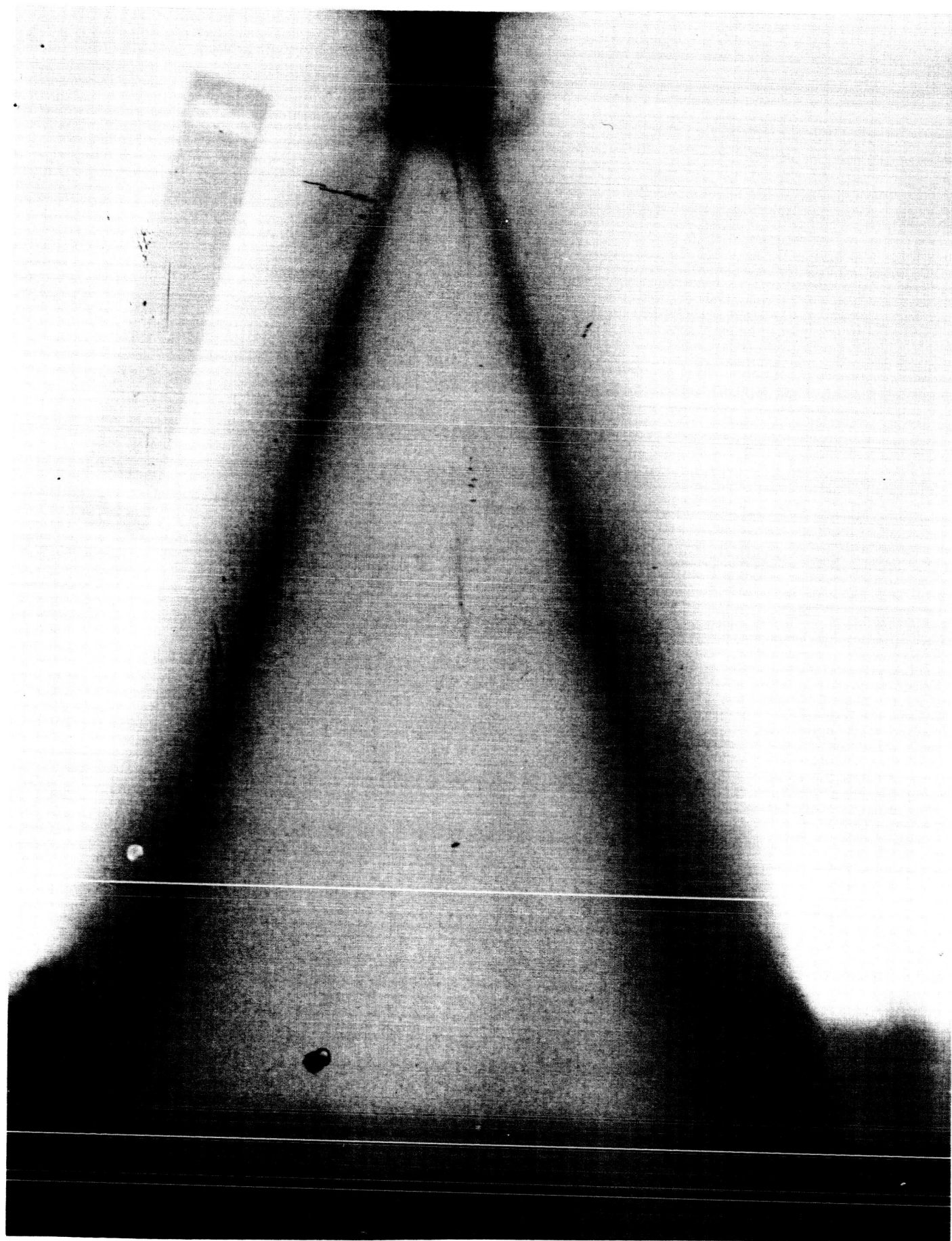


FIGURE 27. SET-UP RADIOGRAPH OF CONICAL SHOT S-3

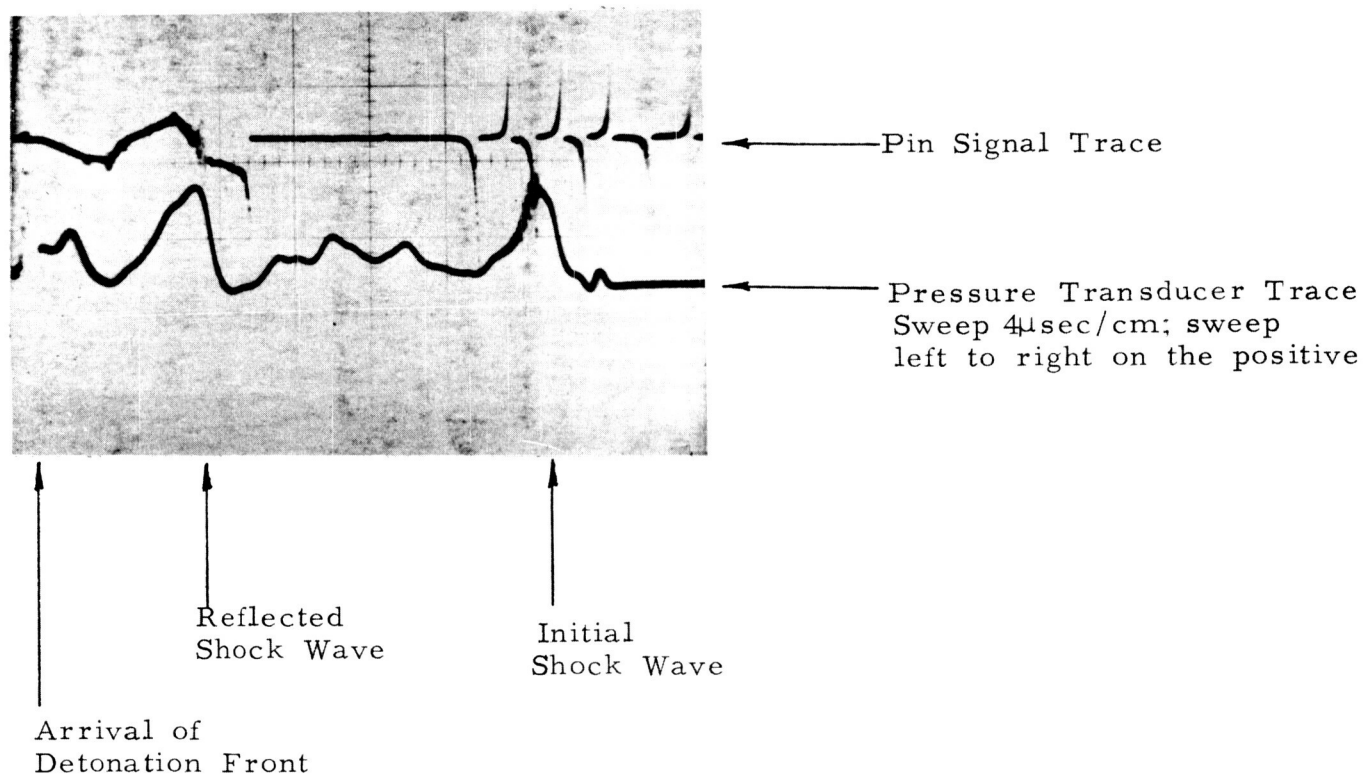


FIGURE 28. TYPICAL PIN-BACKUP AND PRESSURE TRANSDUCER TRACES (SHOT CLG-6)

and an impact switch on the target. The impact switches are reliable, but the muzzle switch is often triggered by gases that move ahead of the projectile in the gun barrel. An additional "make" switch consisting of two layers of 0.002-in. thick aluminized mylar, separated by a 1/16-in. gap, is often mounted in the middle of the range. This switch works very reliably, but it introduces gases and mylar fragments into the pictures taken by the framing camera, so it is used only when considered necessary to provide timing control of auxiliary diagnostics.

A complete history of the flight range is taken with a Beckman-Whitley Model 189A framing camera. This camera takes 24 pictures of interframe times as small as  $0.42 \mu\text{sec}$  with the present 10,000 rps rotor. Exposure time is 1/6 the interframe time. A timing pulse taken from the camera triggers the explosive gun and starts the data recording sequence at what is known as "zero time". The location of the timing pulse prior to zero time can be regulated on the camera so that the first frame is photographed just before the projectile is expected to emerge from the gun barrel. The speed of the camera is regulated to cover the flight of the projectile and the target impact. On shots with some degree of uncertainty, the camera is run relatively slowly to ensure a record of the projectile. On shots where the performance of the gun is fairly reliable, the camera is run at higher speeds to provide more accurate determinations of the projectile velocity. Illumination for the camera is provided by explosively-driven argon candles. A layer of high explosives is detonated at one end of a tube filled with argon. An intense light is generated by the passage of a shock wave through the argon, lasting until the shock wave breaks out the window end of the tube. The time of illumination is regulated by the length of the tube.

The framing camera pictures of the projectile as it initially emerges from the barrel are partially obscured by driver gases carried along by the air flow around and behind the projectile. A definitive picture of the condition of the projectile in flight, as well as one more

reference for determining projectile velocity, is provided by a high-intensity, low-energy pulsed X-ray, called the Bazooka. This instrument was developed by Physics International to provide an X-ray system in an energy range that is not commercially available. It delivers a single, 30-nsec, square-wave pulse in the 30 to 70 kV region, and is portable, occupying about 1.7 ft<sup>3</sup> and weighing about 200 lb, plus the power supply. The tube is an integral part of the unit; it has replaceable electrodes, and requires only an external vacuum pump. The Bazooka is triggered by the muzzle switch, the range switch, or an external time delay. Figure 13 is a radiograph of a nylon projectile which has been accelerated to 4.15 km/sec (shot L-5).

A final and often very definitive source of information is the 6061-T6 aluminum target. An intact projectile will make a single, smooth, spherical crater, whose volume and depth provide further confirmation of the mass and velocity of the projectile. When the projectile is broken or vaporized, the target provides a direct witness to the number of pieces and their relative sizes and velocities. Figure 29 shows the crater from the impact of the intact projectile shown in Figure 13.

## V. EXPLOSIVES FIRING FACILITY

The firing of high explosives at Physics International is done in two steel containment tanks. The tanks are located in an underground secondary enclosure of steel-reinforced concrete block walls, with maze-revetment entrances, and interlocked safety doors. This enclosure joins the main research building where the supporting diagnostic and control instrumentation is located. The enclosure also contains a high explosives assembly room with a ventilated safety box, and mechanical vacuum pumps (Figures 30, 31, and 32). Experiments containing high explosives which exceed the limits of the individual containment tanks are conducted at Physics International's remote test site located near Tracy, California.



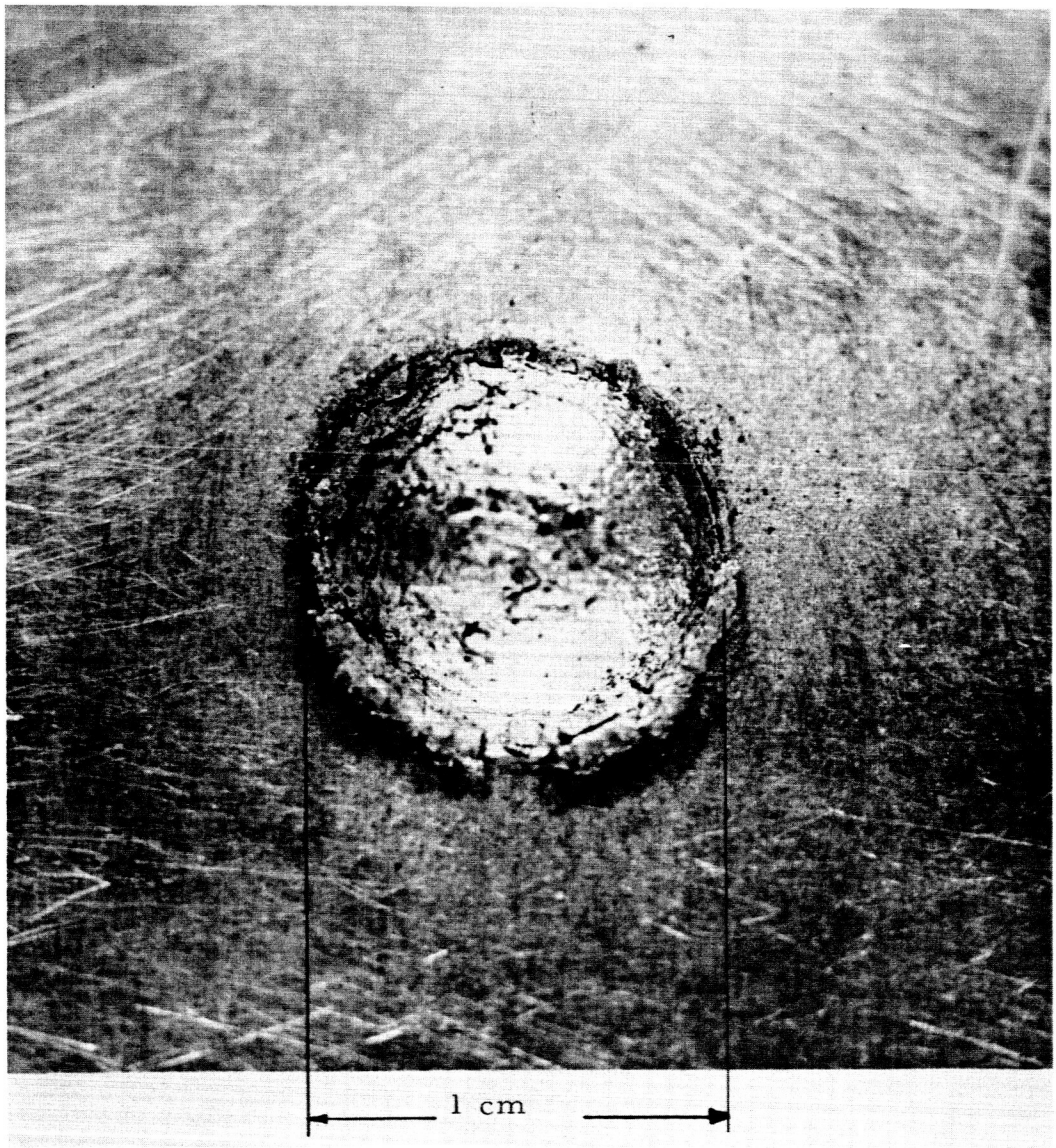


FIGURE 29. CRATER FROM IMPACT OF 4.15 km/sec NYLON PROJECTILE IN ALUMINUM (SHOT L-5)



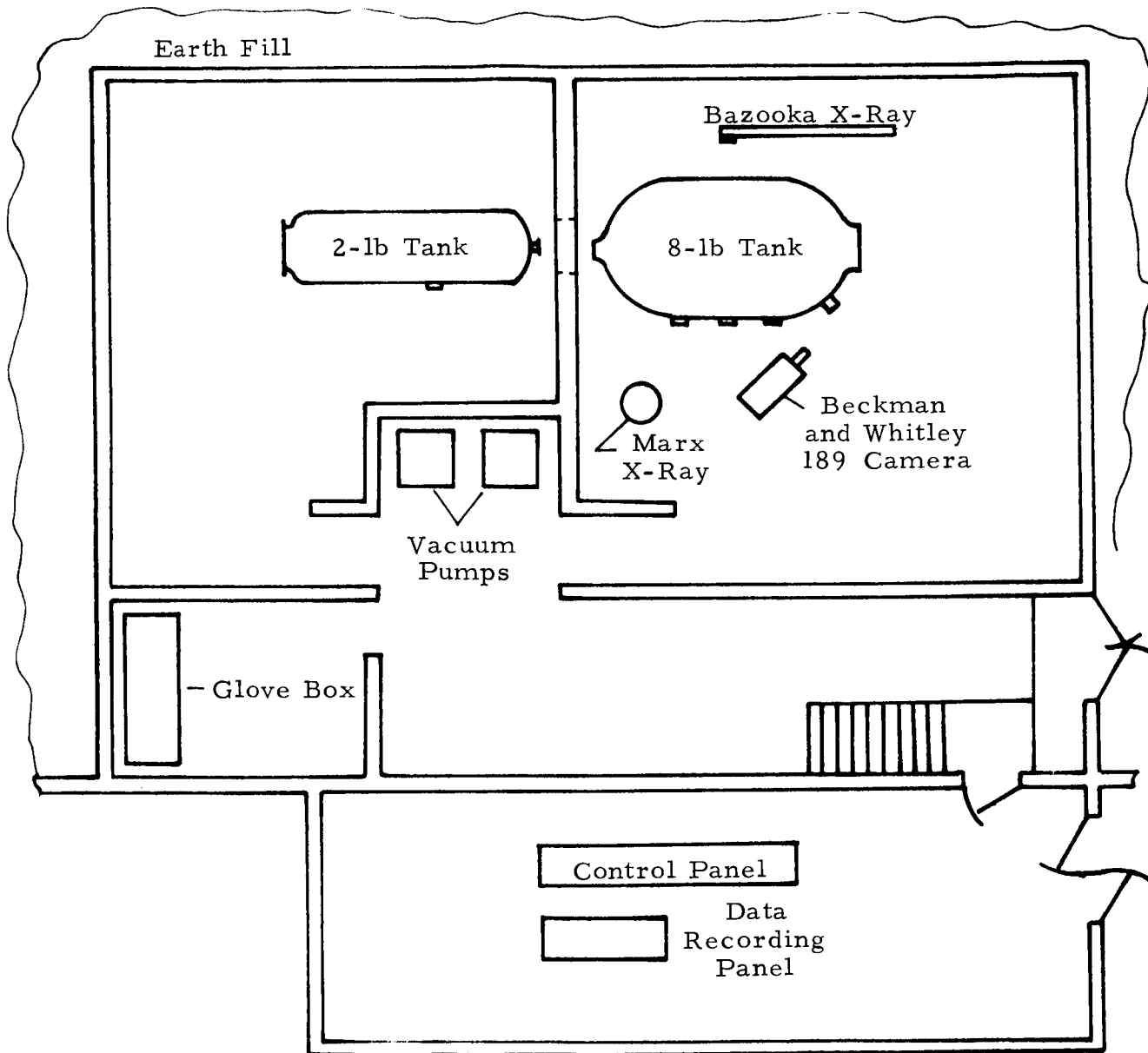


FIGURE 30. HIGH-EXPLOSIVES FIRING FACILITY

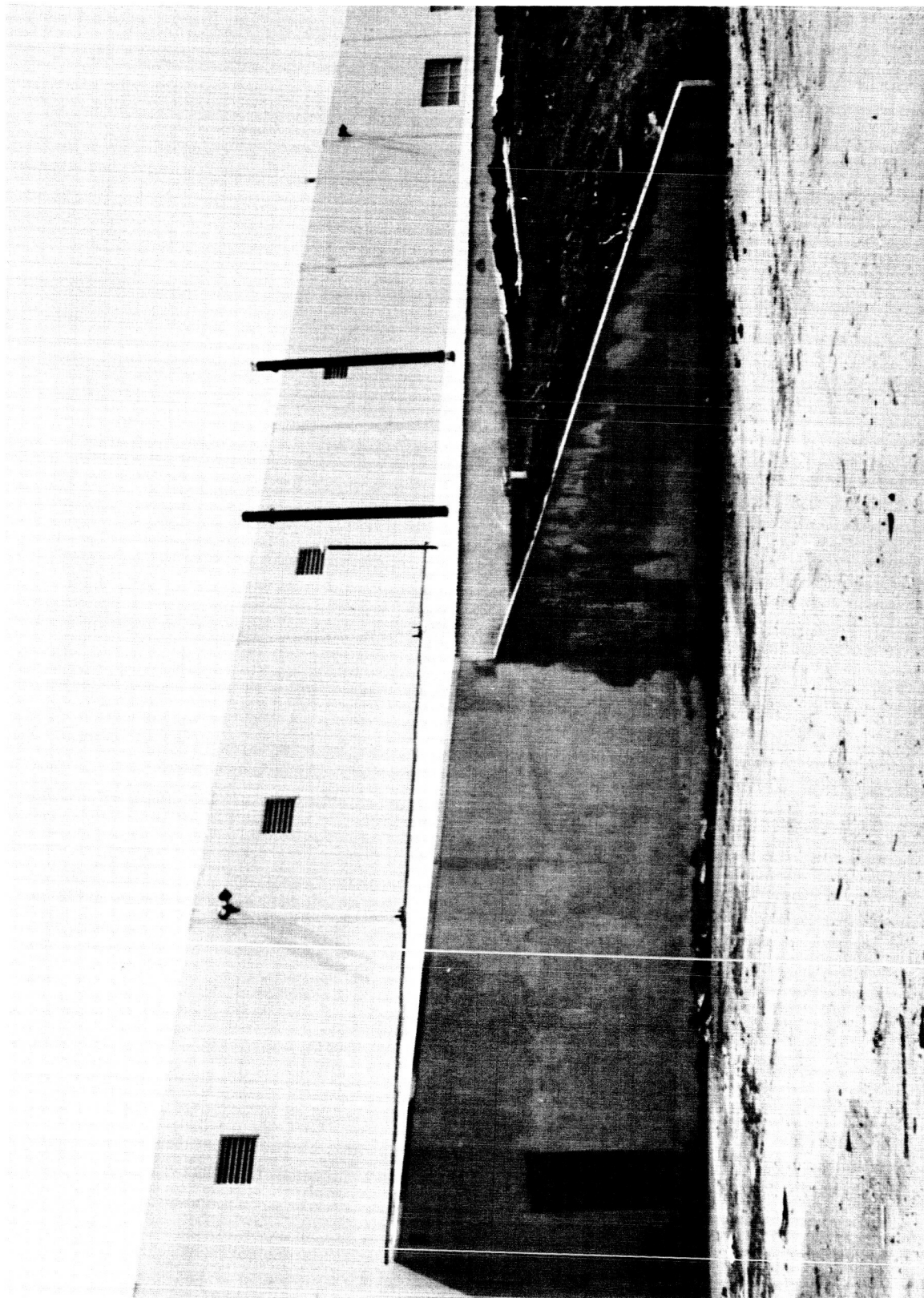


FIGURE 31. EXTERIOR VIEW OF THE HIGH EXPLOSIVES CONTAINMENT FACILITY

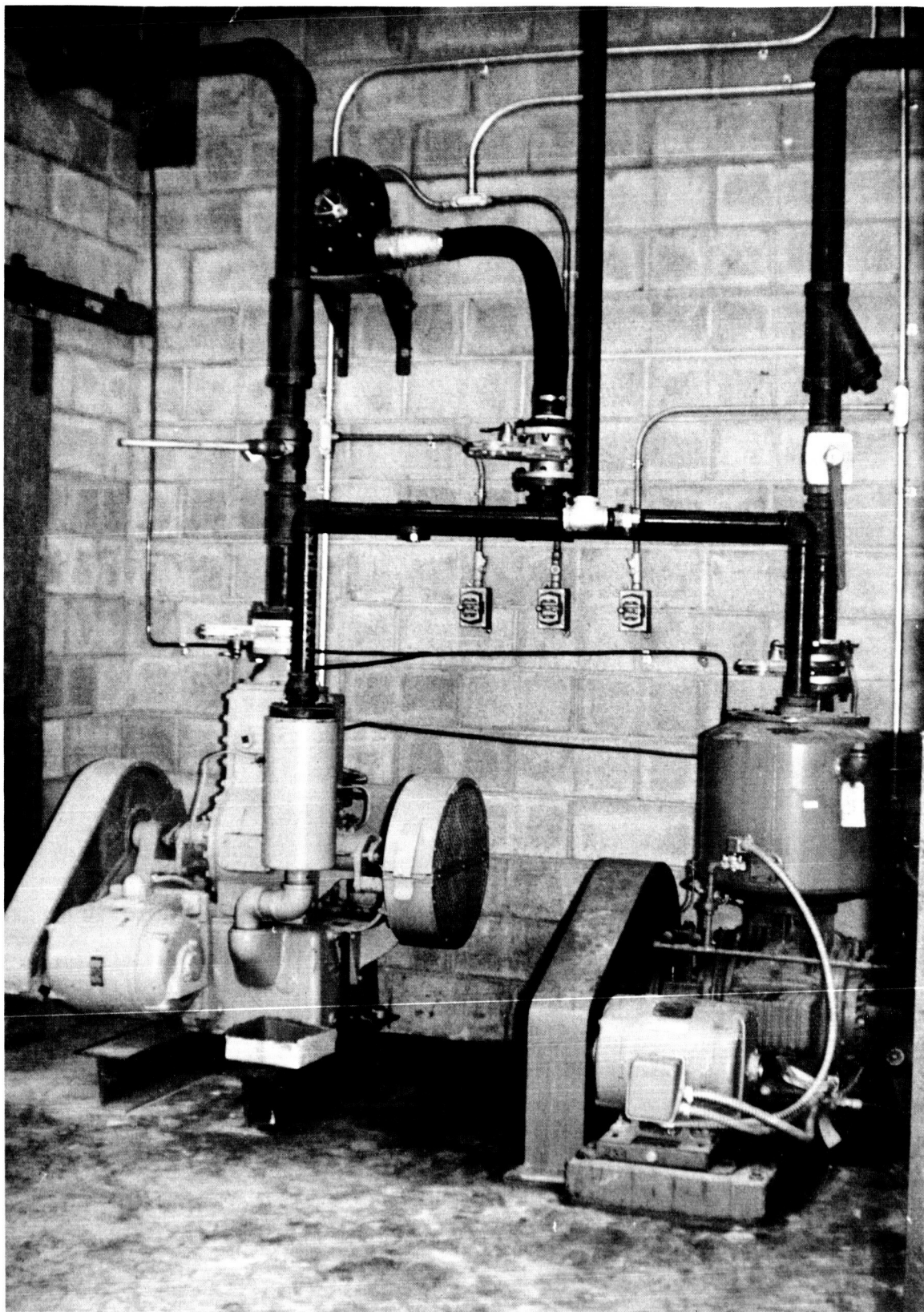


FIGURE 32. VACUUM PUMPS USED TO EVACUATE THE  
HIGH EXPLOSIVES CONTAINMENT TANKS

The primary firing facility is the 8-lb containment tank. This vessel was purchased under the present contract, and greatly facilitates the firing and diagnosis of hypervelocity projectors. Shots up to 8 lb can now be fired with auxiliary instrumentation such as explosive candles and shutters for the framing camera. The design was based on criteria established at the Lawrence Radiation Laboratory, Livermore, California. These criteria state that for  $2 \times 10^4$  psi tensile stress on 1/4-in. thick steel tank wall, the minimum inside radius of the sphere should be  $R = 1.3 \sqrt{w}$ , where R is in feet and w is in pounds of PBX explosive. The final design was a tank 8 ft in diameter by 12 ft long with 1-in. thick walls of ASTM A212-61T grade steel. The design was finished in March, 1964, and contracted to the American Bridge Division of U.S. Steel in South San Francisco, California, for delivery in mid-October, 1964. The vessel was fabricated and inspected in accordance with the ASME Boiler and Pressure Vessel Code. All welds were ground flush to eliminate stress risers, and were radiographed. The entire vessel was normalized to remove internal stresses and then hydrostatically tested for two hours at 550 psi. Fabrication was delayed by the vendor, and the tank was not completed until December 1, 1964. Because of Physics International's rapid growth, it had become necessary to obtain a larger facility in order to maintain efficient operations. The present plant in San Leandro, California, met the requirements of the projected growth rate for several years. Preliminary high-explosive firing permits were issued by the City of San Leandro in November, 1964, and the company immediately issued requests for bids on the construction of the secondary enclosure for the firing tanks. Construction was delayed first because of the moving operations, and then by inclement weather conditions, but was begun in February in spite of rains, and finished by end of March. Figure 33 shows the tank arriving at the firing facility. Figures 34 and 35 are interior and exterior views of the completed facility, with the first shot, Conical Gun L-9, in place and ready to be filled with liquid explosives. This shot was fired on April 16, 1965.

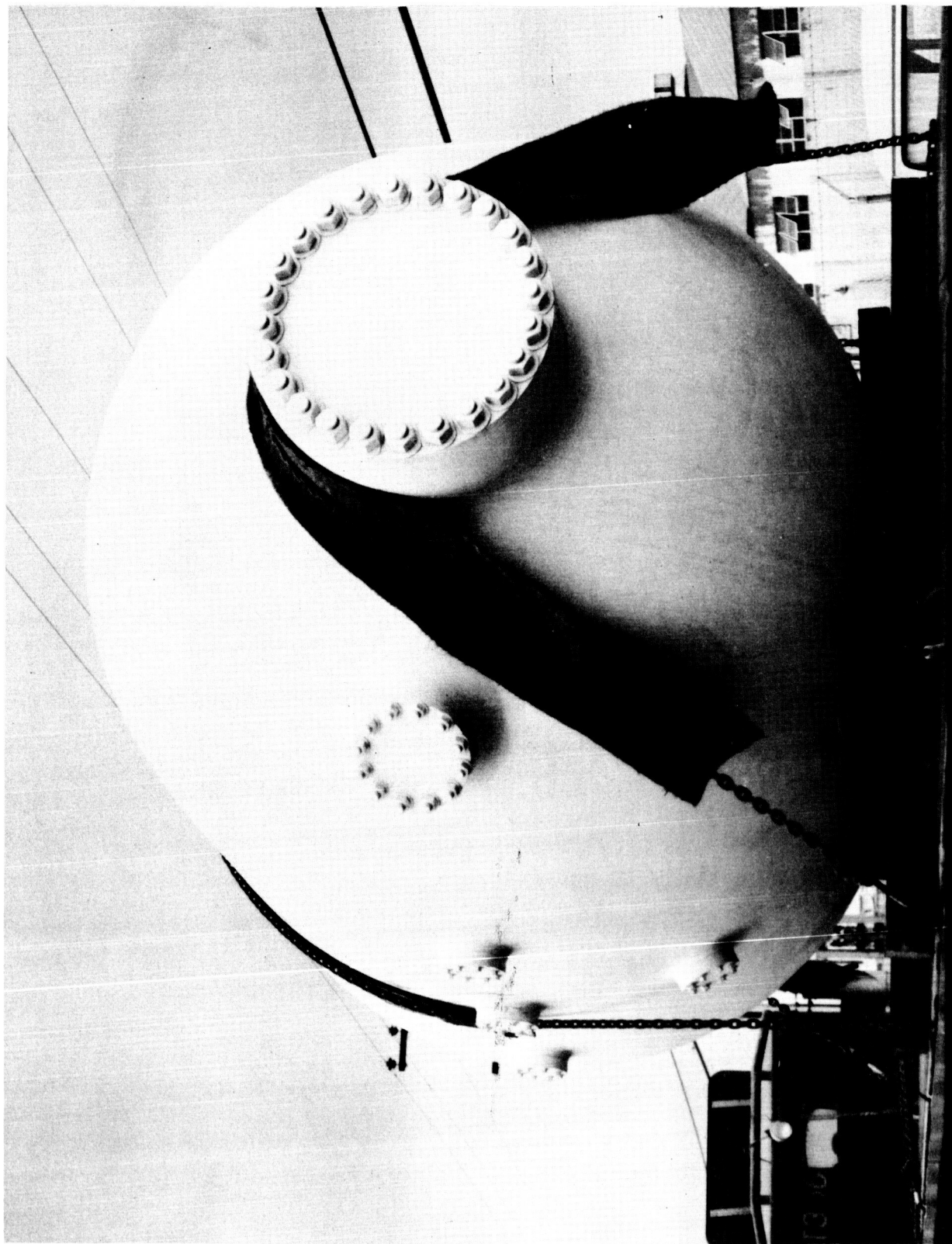


FIGURE 33. 8-lb CONTAINMENT TANK ARRIVING AT HIGH EXPLOSIVES FACILITY



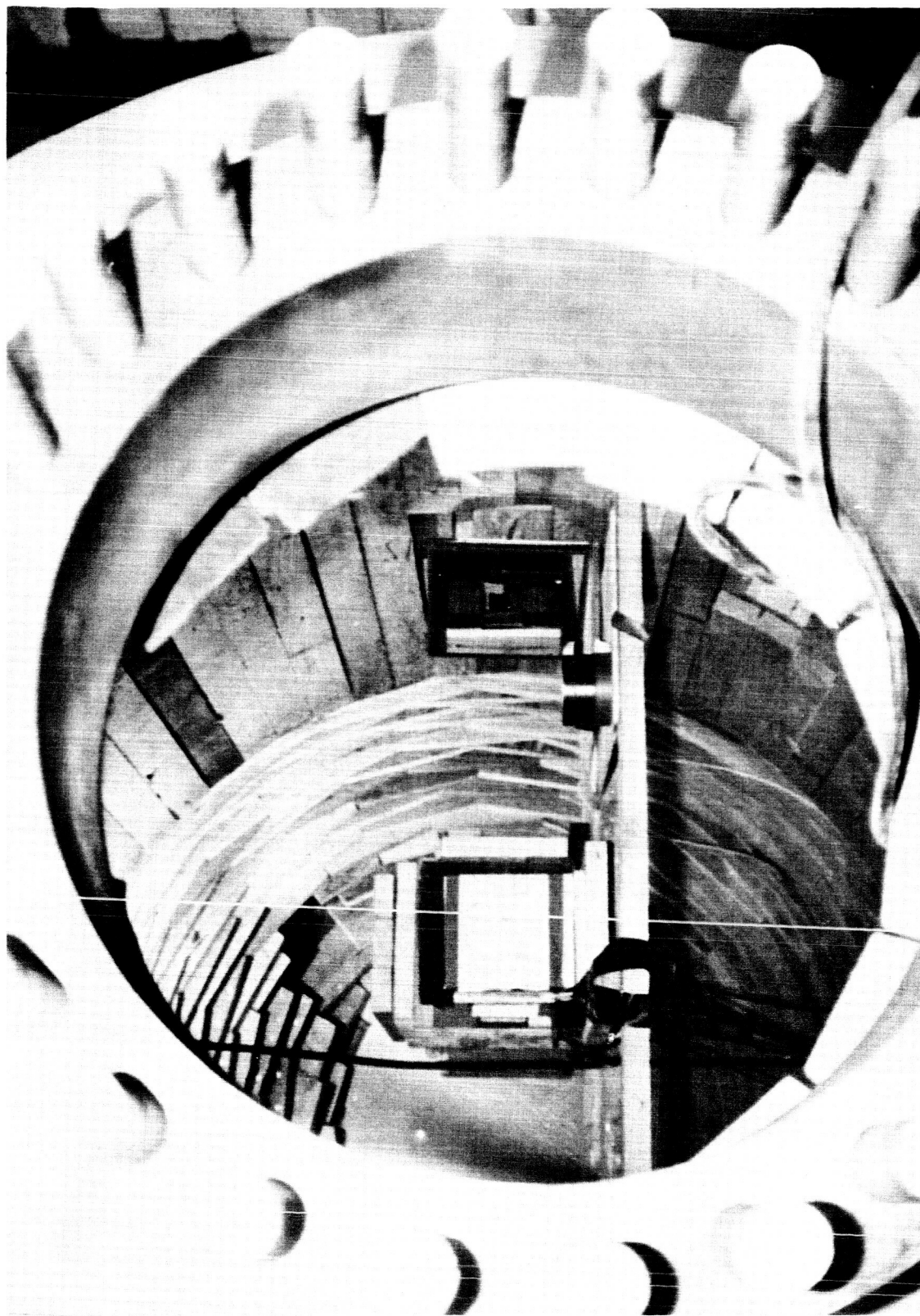


FIGURE 34. INTERIOR VIEW OF 8-1b CONTAINMENT TANK SHOWING THE WOODEN LINING WITH CONICAL SHOT L-9 IN PLACE FOR FIRING

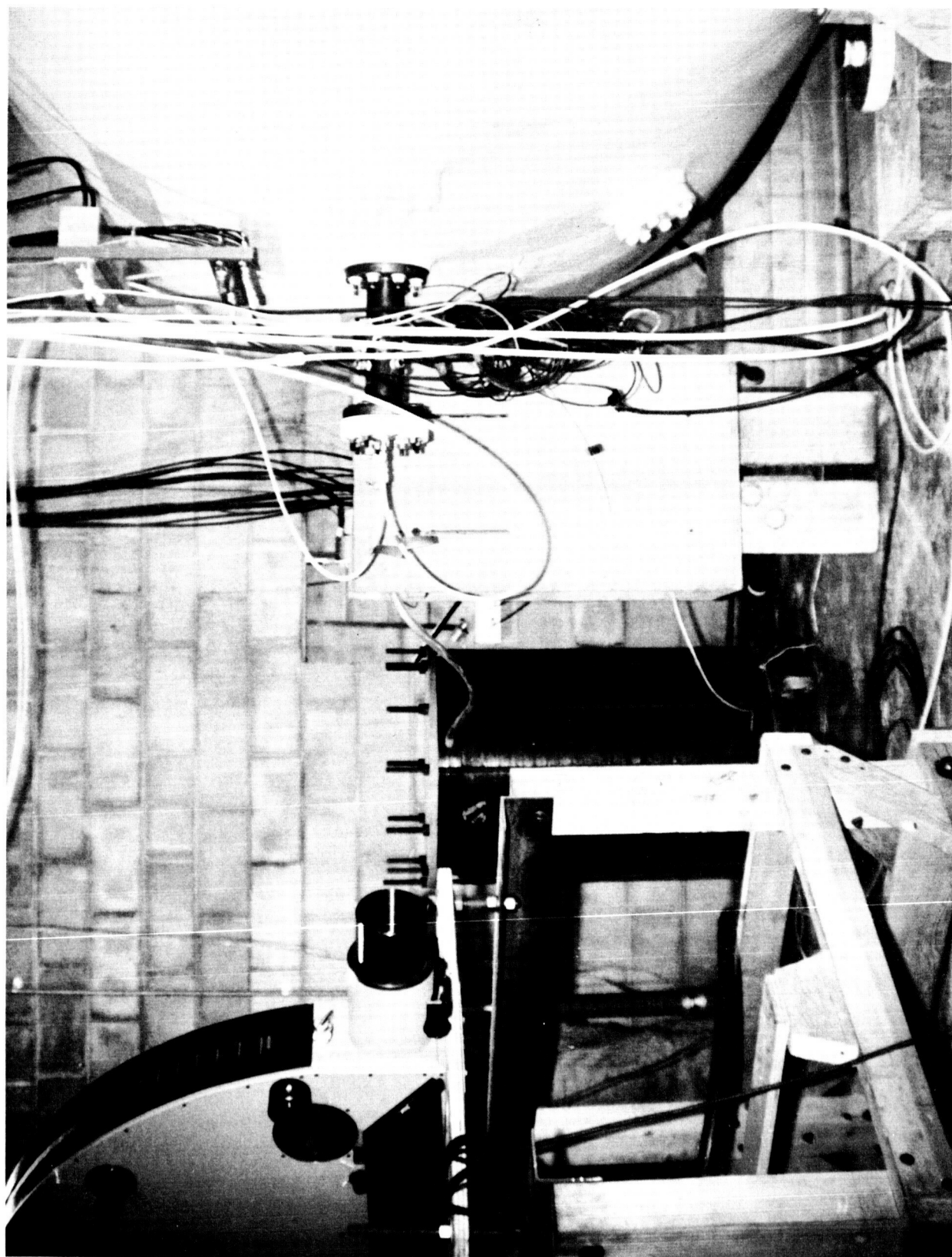


FIGURE 35. EXTERIOR VIEW OF 8-lb TANK WITH DIAGNOSTIC INSTRUMENTATION  
IN PLACE FOR CONICAL SHOT L-9

Explosive charges up to 2 lb can be fired in the smaller tank, and it is presently being connected to the 8-lb tank so that it may also be used for diagnostic techniques that need to be separated or protected from the explosive detonation. For example, the gun may be fired in the 8-lb tank and the projectile launched into the 2-lb tank through a protected tube for controlled atmospheric tests in flight. The adjacent control room contains all the firing control and diagnostic instrumentation that does not need to be directly connected to the containment tanks (Figure 36).



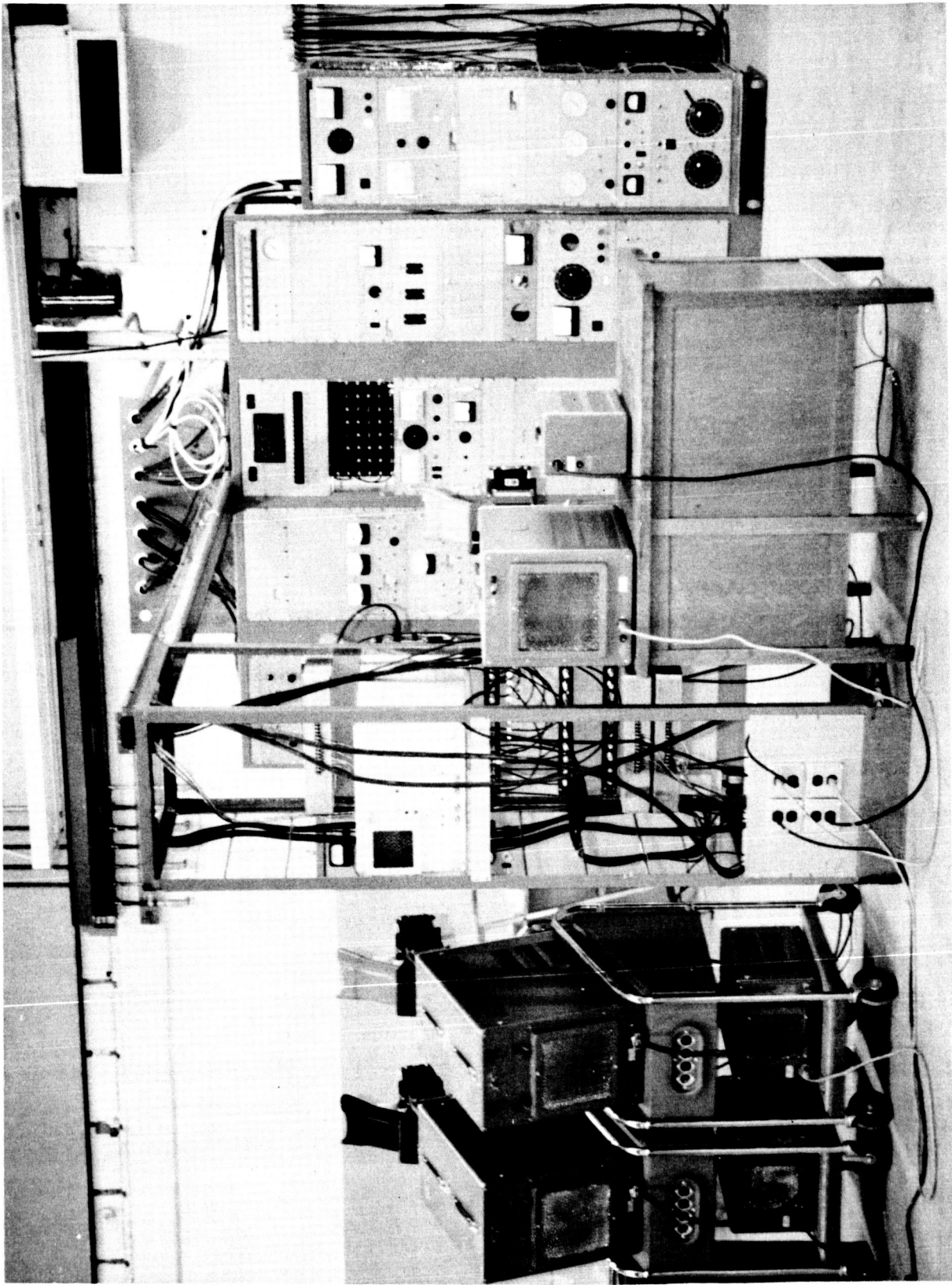


FIGURE 36. CONTROL AND DIAGNOSTIC AREA OF HIGH EXPLOSIVES FACILITY

## VI. CONCLUSIONS AND RECOMMENDATIONS

This work has demonstrated the potential of using high explosive as a primary energy source for hypervelocity projectors. In the past year, explosively driven guns have been developed to accelerate intact 0.1-gm plastic projectiles to 7.9 km/sec. These projectiles are typically accelerated by peak pressures of approximately 20 kb, corresponding to accelerations on the order of  $10^8$  g's. While the maximum tolerable pressure profiles and the most desirable projectile materials have not been determined, high-density polyethylene and nylon appear to be the most satisfactory materials for these accelerations levels.

Much of this effort has been directed toward experimentally verifying the operation of the explosively driven guns. The investigations have demonstrated desirable features that are prerequisites for obtaining even higher projectile velocities:

- (1) High specific energy is available in the high explosive.
- (2) The extremely high gas velocities have ranged from 6 km/sec in the linear gun to 30 km/sec in the conical gun.
- (3) The high gas temperatures, resulting in high sound speeds, act to maintain a more constant base pressure on the projectile.
- (4) The flexibility of design parameters may be varied to tailor the pressure profile at the base of the projectile.

Equally desirable are (1) the low cost of the chemical energy source, (2) the relatively small size of the hypervelocity guns, which are typically 4 ft in length and weigh less than 10 lb, and (3) the compactness and portability of the guns.

The utility of the explosively driven hypervelocity projectors for obtaining even higher velocities depends upon the tailoring of the pressure profile at the base of the projectile. It is recommended that

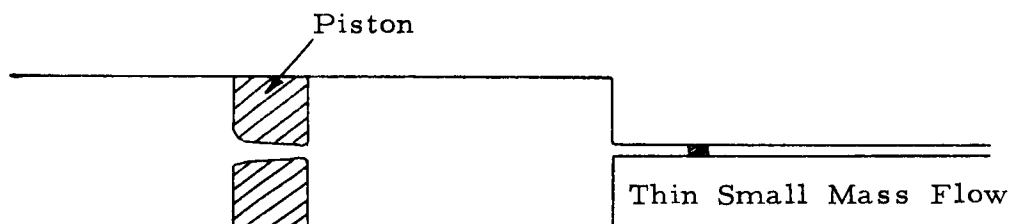
further development be directed toward the control of this base pressure and the systematic determination of the maximum pressure profile that can be tolerated by various projectile materials. It is felt that the concepts developed in this program will be instrumental in extending the presently attainable range of projectile velocities.

## REFERENCES

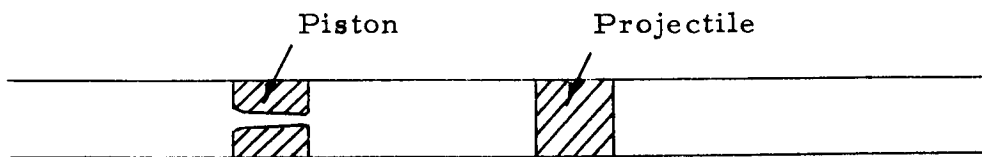
1. E. T. Trigg, and C. Bodin, POD, A One-Dimensional Lagrangian Elastic-Plastic Hydrodynamic Code, Physics International Company, PIER-11, June 1965.
2. C. S. Godfrey, D. J. Andrews, and E. T. Trigg, Pressure Vessel Failure Study, PIFR-190, July 1964.
3. W. S. Koski, F. A. Lucy, R. G. Shreffler, and F. J. Willig, "Fast Jets from Collapsing Cylinders," J. Appl. Phys. 23 (December 1952).
4. J. M. Walsh, R. G. Shreffler, and F. J. Willig, "Limiting Conditions for Jet Formation in High Velocity Collisions," J. Appl. Phys. 24 (March 1953).

## APPENDIX

The "leaky piston" technique shows promise of attaining a rising pressure profile in the reservoir and a relatively high sound speed in the driver gas. This technique, which appears to be novel, was investigated theoretically by Physics International, and is shown schematically in Figure 1. When a strong shock impinges on the piston, it is largely reflected. A controlled amount of gas, however, leaks into the reservoir area. As the pressure in the reservoir builds up, the piston is also accelerated. By the time the pressure is equalized on both sides of the piston, the piston has acquired substantial kinetic energy; the flow of gas through the piston then reverses. At this time, however, the pressure is building up so fast that the reverse flow makes little difference to the pressure build-up.



(a) Reservoir Mode



(b) Constant Area Mode

FIGURE A-1. SCHEMATIC REPRESENTATION OF LEAKY PISTON

The temperature of the gas is increased by being forced through the hole in the piston. This is illustrated in Figure 2, where the piston is assumed to be a stationary orifice. As gas flows through the hole, the system defined arbitrarily by A B C D is compressed to A' B' C D. The work done on this system is  $P$  times the change in volume and must appear as an increase in internal energy of the gas.

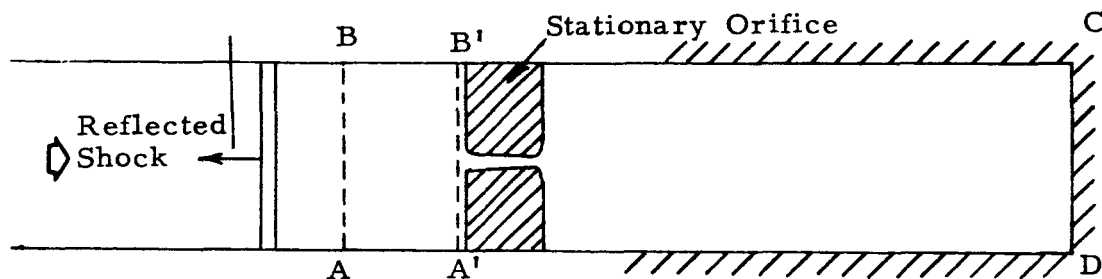


FIGURE A-2. FLOW OF GAS THROUGH STATIONARY ORIFICE

A computer program was coded to investigate parametric changes in the leaky piston design. At present, the program assumes a homogeneous pressure in the chamber. A new program should be completed soon which will also compute the detailed shock history in the chamber. The parameters which must be specified are (Figure 3): (1) conditions of gas at ②, (2) the piston mass ( $M$ ), (3) the ratio of the hole area ( $A^*$ ) to the piston area ( $A$ ), and (4) the length of chamber ( $L$ ).

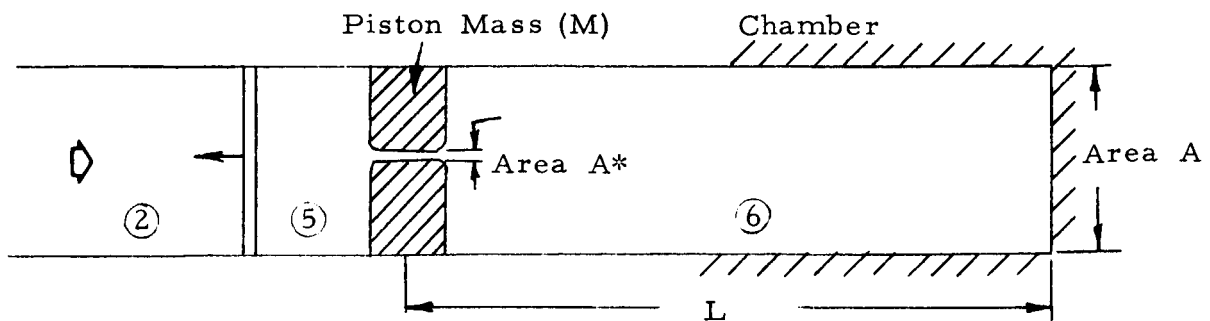
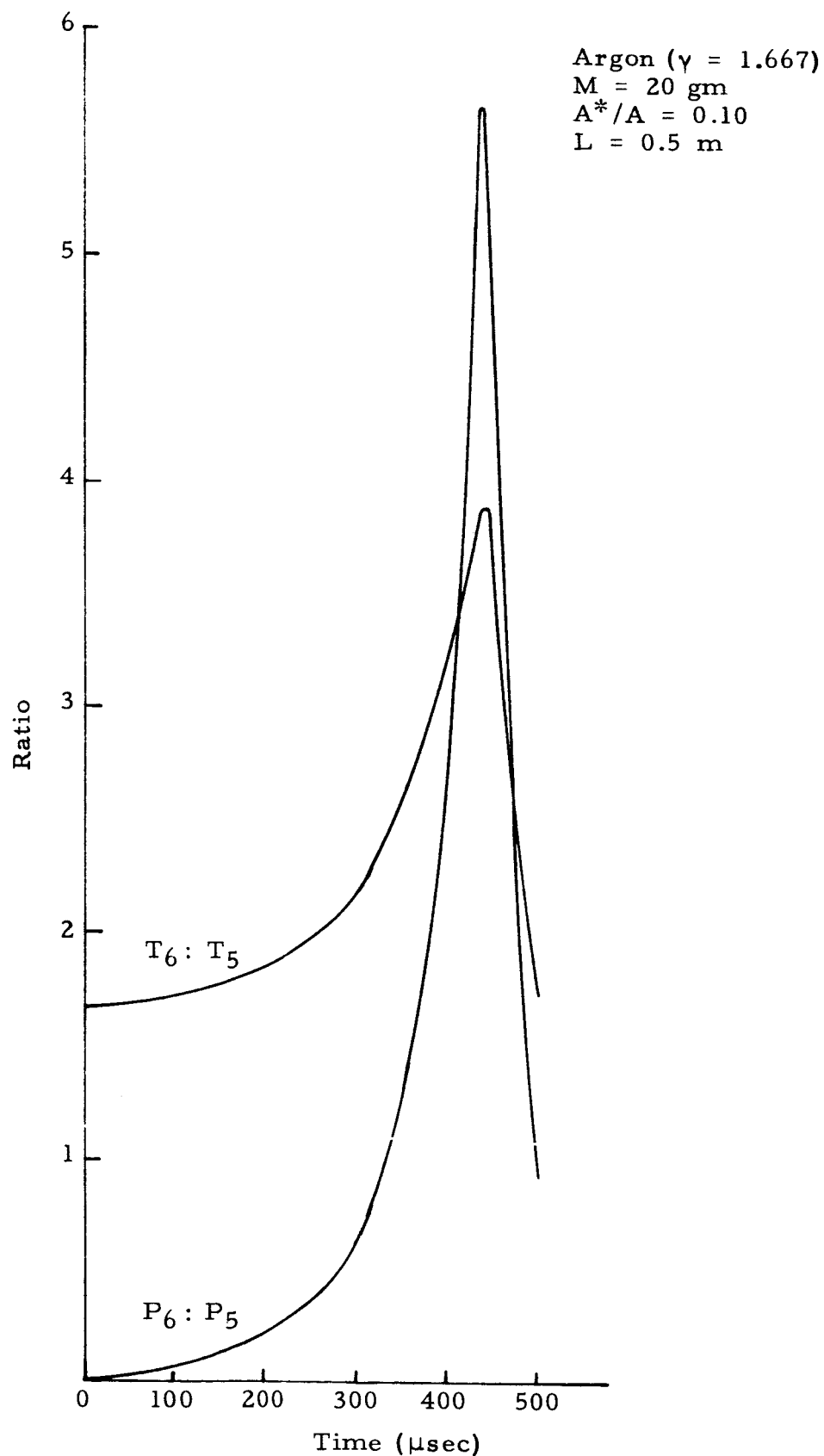


FIGURE A-3. CALCULATIONAL MODEL OF LEAKY PISTON

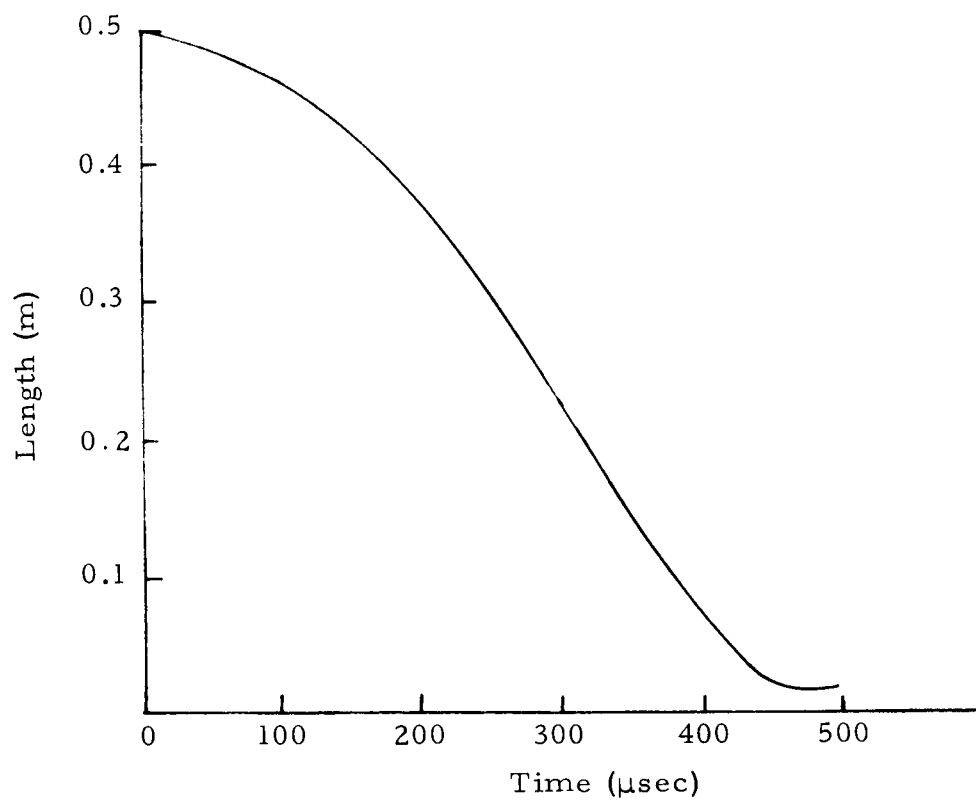
Figure 4 shows the results of a typical calculation. In this case, a Mach 15 shock was assumed in argon at an initial pressure of 100 atmospheres. The argon was considered to be an ideal gas ( $\gamma = 1.67$ ). Values for  $M$ ,  $L$ , and  $A^*/A$  are as noted on Figure 4. The ratio of  $P_6$  to  $P_5$ ,  $T_6$  to  $T_5$ , and the location of the piston are plotted as functions of time. The temperature of the gas rises almost a factor of 4 above the temperature it acquired by reflection at the piston. Likewise, the peak pressure is more than five times that acquired by reflection at the piston. This combination of rising pressure profile and high temperature seems to provide an ideal way to drive the reservoir of a constant-base-pressure gun.



a) Ratio of  $T_6$  to  $T_5$  and  $P_6$  to  $P_5$  as a Function of Time.

FIGURE A-4. RESULTS OF TYPICAL CALCULATION FOR LEAKY PISTON PERFORMANCE





b) Location of Piston Relative to Rear of Chamber  
as a Function of Time

FIGURE A-4. RESULTS OF TYPICAL CALCULATION FOR LEAKY  
PISTON PERFORMANCE